UNIVERSITÀ DEGLI STUDI DI TRIESTE

XXVIII CICLO DEL DOTTORATO DI RICERCA IN NANOTECHNOLOGIE

CANCER CELL MECHANICS AND CELL MICROENVIRONMENT: AN OPTICAL TWEEZERS STUDY

Settore scientifico-disciplinare: FIS/03 FISICA DELLA MATERIA

DOTTORANDO
MUHAMMAD SULAIMAN YOUSAFZAI

COORDINATORE
PROF. LUCIA PASQUATO

SUPERVISORE
DOTT. DAN COJOC

TUTORE
PROF. GIACINTO SCOLES

ANNO ACCADEMICO 2014 / 2015

UNIVERSITÀ DEGLI STUDI DI TRIESTE

XXVIII CICLO DEL DOTTORATO DI RICERCA IN NANOTECHNOLOGIE

CANCER CELL MECHANICS AND CELL MICROENVIRONMENT: AN OPTICAL TWEEZERS STUDY

Settore scientifico-disciplinare: FIS/03 FISICA DELLA MATERIA

DOTTORANDO
MUHAMMAD SULAIMAN YOUSAFZAI

COORDINATORE
PROF. LUCIA PASQUATO

SUPERVISORE
DOTT. DAN COJOC

TUTORE
PROF. GIACINTO SCOLES

ANNO ACCADEMICO 2014 / 2015

Table of Contents

Acronyms

AFM	–	Atomic Force Microscopy
BD	–	Bead Displacement
Ca2+	–	Calcium
DAQ	–	Digital Acquisition Card
d	–	Bead diameter
DIC	–	Differential Interference Contrast
DMEM	–	Dulbecco's Modified Eagle Medium
E	–	Elastic Modulus
ECM	–	Extra Cellular Matrix
EMT	–	Epithelial to Mesenchymal transition
F	–	Force
FA	–	Focal Adhesion
FAK	–	Focal Adhesion Kinases
FCS	–	Fetal Calf Serum
FOB	–	Objective Focus
fL	–	Focal Length
fps	–	frame per second
Id	–	Indentation
IP	–	Interference Pattern
IR	–	InfraRed
k	–	Trap Stiffness
K_B	–	Boltzmann constant
kPa	–	kilo Pascal
mW	–	milli Watt
NA	–	Numerical Aperture
Nd:YAG	–	Neodymium:ytterbium-aluminium-garnet

nm	–	Refractive index of the medium
nN	–	Nano Newton
OT	–	Optical Tweezers
PBS	–	Phosphate Buffer Saline
PDMS	–	Polydimethylsiloxane
pN	–	Pico Newton
PMMA	–	poly(methylmethacrylate)
PSD	–	Power Spectrum Density
QPD	–	Quadrant Photo-Detector
RPMI	–	Roswell Park Memorial Institute
S	–	Slope
SD	–	Stage Displacement
t	–	Time
WD	–	Working Distance
x	–	*Lateral* Displacement
z	–	Vertical component of displacement

Abstract

Since cancer metastasis is a complex process, a lot of research has been carried out to identify different hallmarks for its diagnosis and cure. Mechanical alterations in cancer cells during cell spreading to adjacent tissues and other organs of the body emerged as a prominent hallmark in the last decade.

In this thesis we employed a mechanistic approach based on cell stiffness (elasticity) measurement as a marker to study cell's mechanical response in varying microenvironmental conditions. Mechanical interaction of the cell with the surrounding microenvironment is a blend of cell-matrix and cell-cell interactions. Therefore we adopted an approach to study cells in isolation and in the presence of their neighboring cells, plated on rigid as well as on compliant substrates. The elastic modulus was calculated using the Hertz-model.

We considered three breast cell lines as model, showing three phases of cancer progression: MDA-MB-231, a highly aggressive cell line belonging to the Basal cell-like phenotype; MCF-7, a less aggressive cancer cell line, belonging to the Luminal A cell-like phenotype; and HBL-100, a non-neoplastic cell line, derived from the milk of a Caucasian woman, normal control for breast basal-myoepithelial cells.

Cell elasticity can be locally measured by pulling membrane tethers, stretching or indenting the cell using optical tweezers. We introduce a simple approach to perform cell indentation by axially moving the cell against a trapped microbead. Our scheme is similar to the AFM vertical cell indentation approach and can help to compare the quantitative results and thus complement AFM in a low force regime and loading rates.

The elasticity trend of the three cell lines in isolated conditions showed that the aggressive MDA-MB-231 cells are significantly softer as compared to HBL-100 and MCF-7 cells.

We demonstrate that stiffness measurements are sensitive to the cellular sub-regions as well as the interacting microenvironment. We probed the cells at three cellular sub regions: central (above nucleus), intermediate (cytoplasm) and near the leading edge. Isolated cells showed a significant regional variation in stiffness: higher at the center and fading toward the leading edge. However, the regional variation become statistical insignificant when the cells were in contact with other neighboring cells. We found that neighboring cells significantly alter cell stiffness: MDA-MB-231 becomes stiffer when in contact, while HBL-100 and MCF-7 exhibit softer character.

Furthermore, we have studied the influence of substrate stiffness on cell elasticity by seeding the cells on Collagen and Polydimethylsiloxane (PDMS) coated substrates with varying stiffnesses to mimic extracellular (ECM) rigidities in vitro. PDMS polymer to crosslinker ratio was adjusted to 15:1, 35:1 and 50:1 corresponds to 173kPa, 88kPa and 17kPa respectively. These results show that cells adapt their stiffness to that of the substrate. Compliant substrates lead to reduced cell spreading and cell stiffness. Our results demonstrates that the substrate stiffness influence not only cell spreading and motility, but also cell elasticity.

Finally, from the 3D tracking of the indenting probe, we calculated and compared the elastic moduli resulting from the total and vertical forces for two breast cancer cell lines: MDA-MB-231 and HBL-100, showing that the differences are important and the total force should be considered.

These results lead to the following publications in international peer review journals and an abstract in conference proceedings

1. M. S. Yousafzai, F. Ndoye, G. Coceano, J. Niemela, S. Bonin, G. Scoles and D. Cojoc, Substrate-dependent cell elasticity measured by optical tweezers indentation. *Optics and Lasers in Engineering* **76**:27–33 (2016).

2. Fatou Ndoye, Muhammad Sulaiman Yousafzai, Giovanna Coceano, Serena Bonin, Giacinto Scoles, Oumar Ka, Joseph Niemela, and Dan Cojoc, The influence of lateral forces on the cell stiffness measurement by optical tweezers vertical indentation, *International Journal of Optomechatronics* (accepted 2016 DOI:10.1080/15599612.2016.1149896)

3. G. Coceano, M. S. Yousafzai, W. Ma, F. Ndoye, L. Venturelli, I. Hussain, S. Bonin, J. Niemela, G. Scoles and D. Cojoc, Investigation into local cell mechanics by atomic force microscopy mapping and optical tweezer vertical indentation. *Nanotechnology* **27**: 065102 (2016).
4. Muhammad Sulaiman Yousafzai, Giovanna Coceano, Alberto Mariuti, Fatou Ndoye, Joseph Niemela, Serena Bonin , Giacinto Scoles and Dan Cojoc, Effect of adjacent cells on the cell stiffness measured by optical tweezers indentation, (accepted: *J. biomedical optics,* 2016)

5. Muhammad Sulaiman Yousafzai, Alberto Mariuti, Giovanna Coceano, , Fatou Ndoye, Joseph Niemela, Serena Bonin , Giacinto Scoles and Dan Cojoc, Effect of PDMS as soft substrates on breast cancer cell mechanics, (In preparation, 2016)

6. M. S. Yousafzai, F. Ndoye, G. Coceano, J. Niemela, S. Bonin, G. Scoles and D. Cojoc, Elastic behavior of HBL-100 cells on soft and hard substrates probed by optical tweezers. *10th European Biophysics Congress, Dresden, Germany*, (# L-931, page 48) (2015)

Chapter 1
Introduction

Most of our understanding about cells, tissues and organs, in terms of health and disease, is biochemical in nature. Scientists working in these fields are trying, since decades, to help fight against diseases, especially those which are continuously challenging human lives, such as cancer. The necessity, to broaden the framework of cancer research because of its myriad different faces, shifts the paradigm towards the role of mechanical forces in cellular processes and pathologies to contribute in cancer diagnosis, therapy and cure. A rapidly growing body of evidences indicates that mechanical phenomena are critical to the proper functioning of cells and tissue processes and that mechanical forces can serve as extracellular signals that regulate cell function. Further, any disruption in mechanical sensing and/or function may cause tissue and organ abnormality, such as seen in cancer. This has led to the emergence of a new discipline that merges mechanics and cell biology: cellular **Mechanobiology** (Lim et al. 2010) . This term refers to any aspect of cell biology in which mechanical force is generated, imparted or sensed leading to alterations in cellular function. The study of cellular mechanobiology bridges cell biology and biochemistry with various disciplines of mechanics including solids, fluid, statistical, experimental and computational mechanics (Jacobs et al. 2012).

In vivo, most cells are mechanically and chemically connected to its microenvironment. cell mechanical interaction with the surrounding microenvironment have grasped much attention and witnessed considerable progress (Hoffman and Crocker 2009). Microenvironment is the driving element in cell proliferation (Cheng et al. 2009), viscoelasticity (Suresh 2007; Schoen et al. 2013; Ladoux and Nicolas 2012), functionality (Fu et al. 2010) and cell signaling (Gieni and Hendzel 2008; Jaalouk and Lammerding 2009). There are two types of cell- microenvironment interaction: cell-cell and cell-extra cellular matrix (ECM) interaction. Both of them have prime importance for the fundamental understanding of metastasis and cell behavior in malignant conditions. Mechanical forces from adjacent cells and ECM are transmitted to the interior cytoskeleton of the cell by adhesion junctions (E-cadherins and integrins) and transduced to biochemical reaction.

Cells are able to sense physical factors such as force, geometry and matrix rigidity. This ability of cell has been acknowledged as promising hallmark for cancer phenotyping (Hanahan and Weinberg 2011).

This introductory chapter reviews in detail the mechanical properties of cells. Cancer cell mechanics is explained in detail by introducing, first the mechanical components of cells and their mechanosensitive and mechanotransduction properties leading to cell motility. Detailed literature review has been presented on the modification of mechanical properties of breast cancer cells when they experience different microenvironmental conditions. Substrate rigidity and cell-cells cross talk play a key role in cancer progression and their coordinated signaling decides tissue fate. We highlight the usefulness of optical tweezers (OT) in biomechanics especially to study cell elasticity and alterations in mechanical properties during different environmental conditions. At the end of this chapter, the summary of the thesis is presented.

1.1 Motivation and Goal

The motivation behind the project is the intriguing behavior that cancer cell exhibits at tumoral and metastasis level. Cancer metastasis is the most common cause of death in cancer patients and the main obstacle in cancer treatment. It is now established that metastatic cells are softer than the normal cells, although tumoral tissue is stiffer as compared to normal tissue. Furthermore, metastatic cells exhibit multiple structural alterations during intravasation and extravasation. The transient journey of metastatic cells from primary tumor to the adjacent tissues and other organs of the body exhibits complex modulation of mechanical properties of cells and ECM. Thus, studying the mechanical alterations that cancer cells acquire or induce in the surrounding environment (extracellular matrix (ECM)) at different level of aggressiveness is fundamental to elucidating cancer metastasis. *The goal of this thesis was to develop a force spectroscopy setup (Optical Tweezer (OT)) to study cell mechanics of breast cancer cells in different microenvironmental conditions.* We set the cell stiffness as the principal parameter to study breast cancer cells in on hard and soft substrates as well as in isolated and connected conditions. Cells stiffness on glass and complaint substrates (Polydimethylsiloxane (PDMS) and Collagen) are compared as well as in isolated and connected conditions. The experimental technique reported here is sensitive to force magnitudes of cell-matrix and cell-cell interaction forces *in vivo,* and thus

could detects any elasticity changes in cells when they experience changes in substrate rigidity or when they get in contact with neibhouring cells.

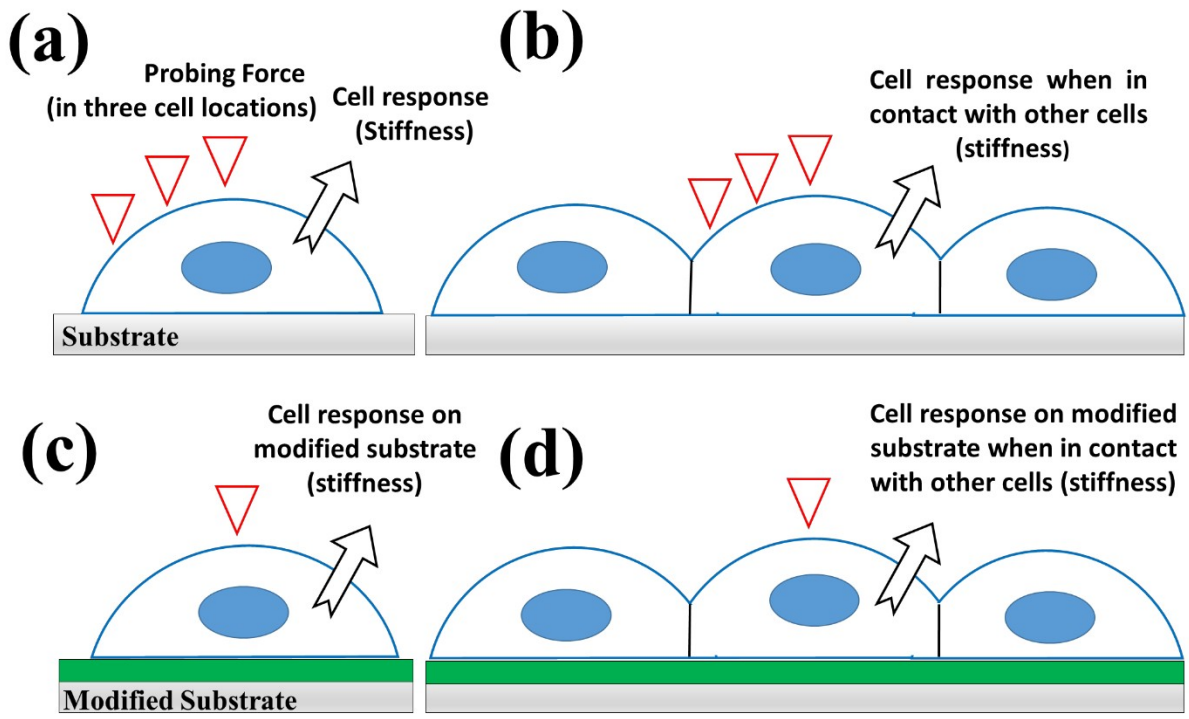

Figure 1.1: Diagram representation of the experimental work. **(a)** Cell mechanical properties were probed at three locations of the cell i.e. center, intermediate location and near the leading edge to understand the mechanical nature of cytoplasm at different cell location. **(b)** When the cell interacts with neighboring cells, the elasticity of the cell changes depending upon the type and level of aggressiveness of the cell. Measuring the stiffness at different locations can give information about the force generating behavior of different kind of cells. **(c)** When the underlying substrate stiffness is modified, the cells response is different as compared to the bare glass substrate. **(d)** Probing cell response in on modified substrate when cell interacts with neighboring cells.

1.2 Cell mechanics and Cancer

Understanding the mechanisms of metastasis formation is in the stage of infancy, in order to disclose the processes regulating the escape of cancer cells from the primary tumors, to migrate and invade neighboring tissues, how they enter (intravasate) into the blood or the lymphatic circulation, how they survive "homelessness" against immune surveillance in the bloodstream, and how they target certain organs to leave (extravasate) the blood circulation and to initiate metastatic outgrowth in specific target organs **(Figure 1.2**).

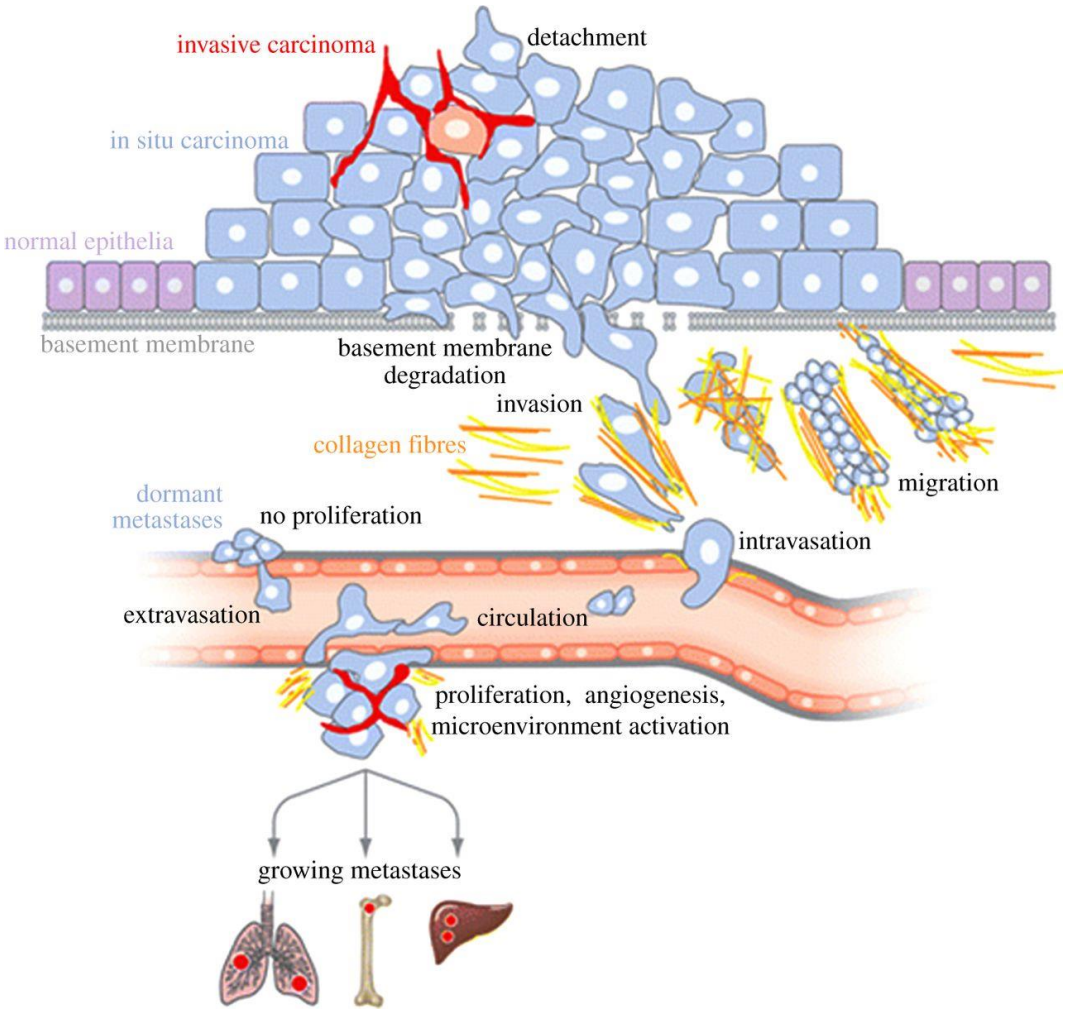

Figure 1.2: Mechanism of metastasis formation. Transformation of normal epithelial cells leads to cell detachment by losing adherens junctions. Degrading basement membrane, tumor cells invade the surrounding stroma, migrate and intravasate into blood or lymph vessels. Cells survived from immune system and flow stresses extravasate and lead to the formation of secondary tumor. (adapted from (Bacac and Stamenkovic 2008))

1.2.1 Cell mechanical architecture

Microtubules, microfilaments and intermediate filaments are the main load bearing components of a cell cytoskeleton and give structural stability to the cell **(Figure 1.3)**. These cytoskeletal constituents along with other cytoplasmic components account for the viscoelastic behaviors of a cell (Suresh 2007). Actin filaments are the most prominent components of cell cytoskeleton (Pollard and Cooper 2009). The process of actin polymerization and depolymerization makes the cell responsive to external stress. The cell stiffness, a widely measured property for cell

viscoelastic characterization, can be viewed at molecular level as actin/myosin perturbation and cytoskeletal deformation (Ketene et al. 2012).

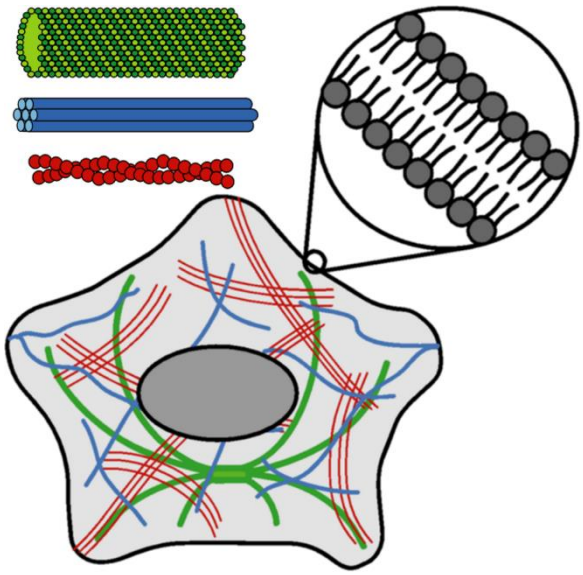

Figure 1.3: Cell architecture is composed of Actin filaments (parallel filaments, in red), intermediate filaments (wavy filaments, in blue), and microtubules (thick filaments, green). The mechanics of a cell is also defined by its membrane (cell border), nucleus (oval), and cytoplasm (region between membrane and nucleus) (adapted from (Rodriguez et al. 2013)).

1.2.2 Cell mechanical architecture and exterior world

The cell cytoskeleton is connected to the exterior world i.e Extracellular Matrix (ECM) and neighboring cells through cross membrane receptor (Integrins) and junction proteins (E-cadherins) respectively as shown in **Figure 1.4** (DuFort et al. 2011). Cells anchorage on the ECM is dependent on Focal Adhesion (FA). FA's are highly dynamic and mechano-sensory complexes composed of integrins, Vinculin, Talin, p130Cas, FAK and SrC which provide a link between cell cytoskeleton and ECM. Focal adhesion serve as conduit through which signal transductions occurs in response to physical forces (Ingber 2006; Bershadsky et al. 2003).

The ECM provides a scaffold to cells and is a principal component of tissues and organs. It constituted of molecular components like Collagens, Elastins, Proteoglycans, Fibronectin and Laminin that regulates number of cellular processes including cells adhesion, migration, apoptosis, proliferation and differentiation (Vogel and Sheetz 2006; Suresh 2007; Hoffman and Crocker 2009). ECM is responsible for all biochemical and biomechanical intercellular signaling. Perturbation in this network could causes the loss of cell and tissue homeostasis and lead to number of diseases, including cancer (Mierke 2014; Wirtz et al. 2011; Ingber 2008; Bissell and Hines 2011).

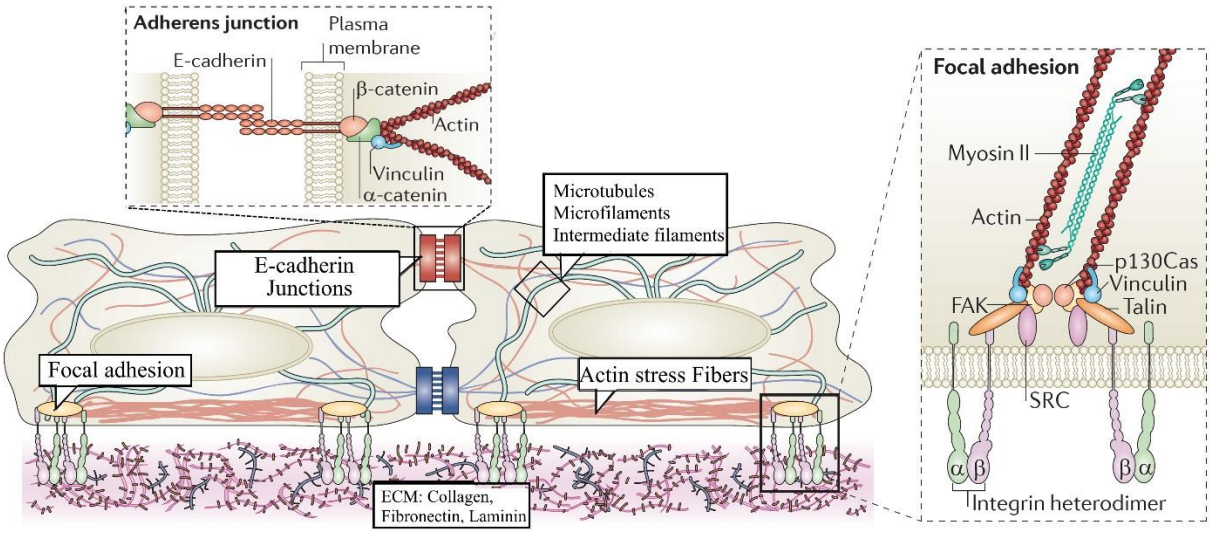

Figure 1. 4: The cross membrane integrins connects the cytoskeleton of the cell to ECM proteins such as collagen or fibronectin. The mechanical and mechano-chemical properties of all these components and their interconnectivity determine the rigidity-sensing process (adapted from (DuFort et al. 2011)).

1.2.3 Mechanosensitivity and mechanotransduction in cell

Cells are capable of sensing mechanical stimuli and translating them into biochemical signals, this ability allows cells to adapt to their physical surrounding by remodeling their cytoskeleton, activating various signaling pathways and changing their gene expression (Ladoux and Nicolas 2012). These phenomena are governed by two processes - mechanosensing and mechanotransduction. Mechanotransduction refers to the conversion of mechanical forces into biochemical or electrical signals that initiate structural and functional remodeling in cells and tissues. Processes like auditory, blood flow regulation in circulatory system, lung expiration and inspiration, muscles & bone remodeling and sense of balancing are physiological mechanosensation originated in response to force, pressure and flow speed.

The magnitudes of forces that cells encounter in vivo might not be sufficient to activate a particular mechanosensor (e.g., molecular unfolding, and change in conformation) for changes in their biochemical activity (Vera et al. 2005). However, channeling of forces along discrete molecular filament networks (e.g., ECM, cytoskeleton) provides a way to concentrate stresses on specific molecules at particular locations while protecting most other cellular components from these same

mechanical forces. In this manner, only a subset of mechanosensory molecules will experience force levels high enough to alter their biochemical activities.

External forces may activate the actin-myosin motor machinery for cell spreading and locomotion (Pollard and Cooper 2009; Hu et al. 2004) while some studies have shown that external forces transmitted to the cytoskeleton can cause rupture of microtubules, which in turn can initiate a biochemical signaling response (Odde et al. 1999). Forces applied via membrane receptors are transmitted to cytoskeleton to the nuclear envelop, via lamin, and then to chromatin, causing nuclear deformation and gene transcription (Maniotis et al. 1997). It is shown that the overall cell shape and geometry respond to local forces over time, and the integration of those responses, have an important role in the regulation of gene expression. Transcription factors that are recruited to the adhesion sites could have an important role in translating the physical stimulus that is sensed at the periphery into biochemical signals that alter gene expression. Many mechanosensitive molecules at FA like paxillin (Woods et al. 2002; Turner 2000), zyxin (Cattaruzza et al. 2004) are translocated to the nucleus and in turn change gene transcription. This mechanism offers an evident way to transform force on specific intracellular-adhesion sites to a change in protein expression. Recent studies using microarray also confirm that changes in cell shape correlate with several changes in gene expression (Dalby et al. 2005). Mechanotransduction and mechanosensing mechanisms demand more rigorous studies to ascertain how external forces of such small magnitudes (~ pN) activates signals which are integrated by multiple proteins in focal adhesion and cytoskeleton to produce a coordinated biological response.

1.2.4 Mechanism of Motility

Cancer cells may use a broad repertoire of cell migration and invasion, and exhibit multiple dynamical changes i.e remodeling their cell-cell and cell matrix adhesion and their actin cytoskeleton, reorganize its molecular processes that involve in various signaling networks (Bershadsky et al. 2003). Cell migration can be classified into single cell (mesenchymal, amoeboid) migration or collective cell (sheet, strand, tube, clusters) migration. The types of migration is dependent on the extracellular protease activity, integrin mediated cell matrix adhesion, cadherins mediated cell-cell adhesion, cell polarity, and cytoskeleton rearrangements. Morphogenic processes are utilized to control their migrator capabilities like dramatic reorganization of the actin cytoskeleton and the associated formation of membrane protrusions

required for cell motility in three dimensional environment, including lamellopodia, filopodia, podosomers and invadopodia.

Based on their central function in actin remodeling, cell proliferation and survival, RhoGTPases play an important role in tumor cell invasion and metastasis (Hall 2005; Ridley 2006). RhoA, Rac1 and Cdc42 are the best studied members of the RhoGTPase family, having critical role in cell migration and invasion (Wojciak-Stothard and Ridley 2003; Narumiya et al. 2009; Vega and Ridley 2008; Sahai and Marshall 2002; Jaffe and Hall 2005). In context of cell migration RhoA induces actin stress fibers formation and regulates cytoskeletal configuration affecting cell-cell and cell-matrix adhesion. Conversely, Rac1 is involved in lamellopodia and membrane ruffle formation, and Cdc42 excites filopodia formation (Liu et al. 2010). The tight regulation of actin cytoskeleton remodeling is not only critical for cell motility but also for other cellular processes, such as endocytosis and intracellular trafficking (Yilmaz and Christofori 2010).

On the basis of morphological and functional differences, single cell migration has two modes of migration i.e. mesenchymal cell migration and amoeboid migration. Cancer cells can acquire either one or mixture of both strategies. Mesenchymal cell's movements is driven at the leading edge, by Rac-induced cell protrusions and actin polymerization in cortical cables and stress fibers. These cells remodel the extracellular matrix by proteolysis (Lo et al. 2000; Raeber et al. 2008).

In contrast amoeboid cell migration is used by round cells, which in a push –to-squeeze type of migration make their way through the extracellular matrix. Their movement is driven by RhoA/ROCK-mediated bleb like protrusions regulated by active myosin/actin contractions and cortical actin polymerization. The ECM is remodeled only by mechanical forces in the absence of significant proteolytic activity and cell migrates through the small pores of ECM (Brunner et al. 2006; Wolf and Friedl 2006). These cells migrate rater fast as compared to mesenchymal migration.

In contrast, collectively migrating cells maintain their cell-cell junctions and migrate in sheets, strands, tubes, and clusters, either still in connection with their originating tissue or as separated, independently migrating clusters (Friedl and Gilmour 2009; Friedl et al. 2004). There are only few differences to solitary migrating cells when viewed from cellular level. Collectively migrating cells also form membrane protrusions, such as ruffles and pseudopodes; they use cell-matrix adhesion receptors, such as β1-integrin and β3-integrin, to form focal adhesions connected to the actin cytoskeleton; they direct proteolytic breakdown of the extracellular matrix to generate a path

through the matrix scaffold; and they use the actin-myosin contractile apparatus for local contraction and cell movement. Yet, in contrast to their solitary migrating counterparts, collectively migrating cells do not retract their cellular tails but rather exert pulling forces on neighboring cells that are connected by adhesion junctions. Thereby, cells keep in most, but not all, cases their position in the collective.

1.2.5 Mechanical Phenotypes of Cancer cells

It is now established that mechanical parameters can be used as biomarkers to classify cancer cells phenotyping (Paszek et al. 2005; Huang and Ingber 2005; Remmerbach et al. 2009). Change in cell elasticity, deformability and traction forces are the most studies mechanical phenotypes used to differentiate cancerous cells from normal ones (Kraning-Rush et al. 2012; Guck et al. 2005; Coceano et al. 2016; Tavano et al. 2011). A large number of experiments on cells shows that cells mechanical response is viscoelastic, having both elastic and viscous behavior (Nawaz et al. 2012). To elicit biomechanical response of cells, a variety of experimental techniques like micropipette aspiration, magnetic tweezers, optical stretchers, AFM and optical tweezers have been established capable of applying and measuring force magnitudes sufficient for cells mechanical phenotyping. Here our focus is on the study of cell mechanical properties, specifically cells' resistance to deformation due to applied forces using optical tweezers.

1.3 Cell mechanics and cell microenvironment

Microenvironmental biochemical and physical stimuli activate many cellular processes such as stiffening, softening, maturation, ion influx, morphological changes, generation of tractions forces or focal adhesions (Discher et al. 2005). During normal growth, these stresses and responses are highly regulated and coordinated in both space and time to cooperatively guide the proper development of tissue structure and function and, ultimately, of the organism. When these cues are disturbed by pathological stimuli, this imbalance can trigger maladaptive reorganization of the cytoskeleton leading to abnormal tissue growth and diseases such as cancer (Subra Suresh, 2007; Makale, 2007), atherosclerosis and malaria (Park et al., 2008).

Cancerous ECM (and hence tissue) exhibits higher stiffness compared to its normal counterpart and this elevated stiffness is partly responsible for the critical process of cancer cell migration and

invasion (Ingber 2008; Friedl et al. 2004; Lo et al. 2000; Bissell and Hines 2011). Similarly, it is know that invasive cancer cells are softer as compared to normal cells (Coceano et al. 2016). However, the relationship between the mechanical properties of the ECM and the intracellular mechanical properties that influence cell migration is still not well understood.

1.3.1 Effect of substrate on cell stiffness

Mechanical interactions between tissue cells and ECM have grasped much attention as they play an important role cancer progression and invasion. Cell constantly sense and respond to the stiffness (rigidity) of its ECM (substrate). In various processes including tumor progression or tissue development, the stiffness of the ECM is modified (Georges and Janmey 2005; Paszek et al. 2005). Cell sense the rigidity of the substrate and can migrate toward increased stiffness (Discher et al. 2005), by the mechanism of called Durotaxis [1], as shown in **Figure 1.5**. Cells favor stable substrate adhesions (Carter 1967), which depends on substrate rigidity (Pelham and Wang 1997; Giannone et al. 2004; Chan and Odde 2008).

In lab-based experiments, cell are seeded on glass substrate having higher elastic modulus ($E \approx$ GPa). In the last two decades, surface modification methods using polymer hydrogels (polyacrylamide (PA), PDMS) are extensively used to obtain surfaces with varying elastic moduli (from 100Pa to 100kPa) to mimic ECM rigidities in vitro (Khademhosseini 2008). Pelhem *et. al*. examined normal rat kidney epithelial and 3T3 fibroblastic cells on a collagen coated polyacrylamide substrate with distinct elasticity, while maintaining a constant chemical environment.

Flexible substrates showed reduced spreading and increased rates of motility or lamellipodial activity as compared with cells on rigid substrates. Fluorescent images of adhesion proteins such as vinculin revealed that on soft, lightly cross-linked gels ($E \approx 1$ kPa), irregularly shaped and highly dynamic adhesion complexes were observed whereas stiff, highly cross-linked gels ($E \approx 30–100$ kPa) induced FA's with normal morphology and much more stability, close to those

[1] Durotaxis is a form of cell migration in which cells are guided by rigidity gradients, which arise from differential structural properties of the extracellular matrix (ECM). Most normal cells migrate up rigidity gradients (in the direction of greater stiffness)

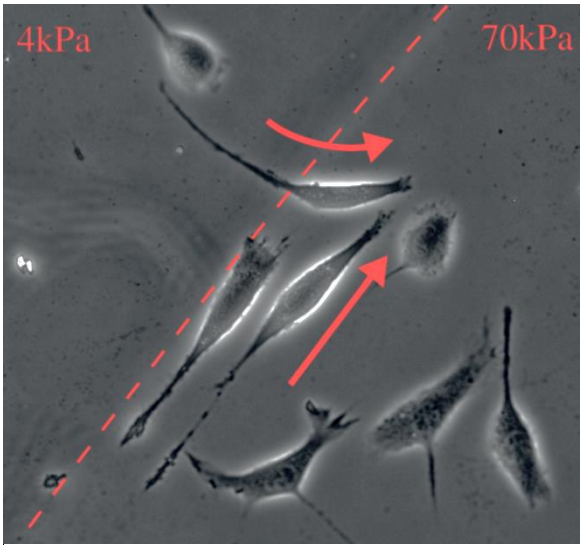

Figure 1.5: Cells feel the mechanical properties of the ECM. When plated onto an ECM that consists of adjoined rigid and soft regions, fibroblastic L cells move from the soft part to the rigid one, while cells on the rigid region remain confined in this region.(adapted from (Ladoux and Nicolas 2012)).

observed in cells cultured on glass substrates (Pelham and Wang 1997). The possible reasons could be that the reduced stress on soft substrates could impact on the maturation of FAs. In fact, traction force mapping of fibroblasts on gels proves that stiffer substrates are pulled harder as compared to softer substrate (Lo et al. 2000). If a cell can generate higher traction, it has some internal structure that can sense the stiffness of the matrix on which it resides. Studies shows that contractile acto-myosin apparatus can act as a global rigidity sensor (Kobayashi and Sokabe 2010).

Experiments on mesenchymal stem cells have shown that they can differentiate toward neurons, myoblasts and osteoblasts on PA gels of different stiffnesses with identical biochemical conditions (Engler et al. 2006). It has also been reported that cell adopts a more rounded morphology on soft substrates and more flattened on stiff ones (Pelham and Wang 1997, Ghibaudo *et al* 2008, Tee *et al* 2011) as shown in F**igure 1.6**. It seems that cell contractility could be modulated by the internal cytoskeletal stiffness via a higher polarization of actin filaments. Tissue cells also has the ability to tune their internal stiffness to match that of their substrate (Solon et al. 2007) which make cells to migrate and helps in wound repair.

The cytoskeleton of a cell is prestressed because tensional forces that are generated within contractile microfilaments and spreaded throughout the cell are balanced by internal microtubules that resist being compressed, as well as by extracellular adhesions to ECM and to other cells (Kumar et al. 2006; Wang et al. 2001; Ingber 2003; Hu et al. 2004). This allows cells to shift compressive forces back and forth between microtubules and ECM adhesions, such that microtubules bear most of the pre-stress in rounded cells with few anchoring points whereas the

ECM bears most of the load in spread cells on highly adhesive substrates (**Figure 1.6**) (Hu et al. 2004). The existence of this complementary force balance in the cytoskeleton explains how external forces that are applied at the cell surface can alter the chemical potential of tubulin and thereby control microtubule polymerization in cells as is required for nerve outgrowth or directional cell migration, as well as why cytoskeletal tension and ECM adhesions contribute to this response. Similar mechanical interactions between microfilaments, microtubules, and cell substrate adhesions govern the shape and stiffness of the cells and their linked ECMs ((Pollard and Cooper 2009)). In general , the tensional forces are supported by actin (Wang et al. 2002), and intermediate filaments (Wang and Stamenović 2000), whereas compressive forces are supported by the microtubules and adhesions..

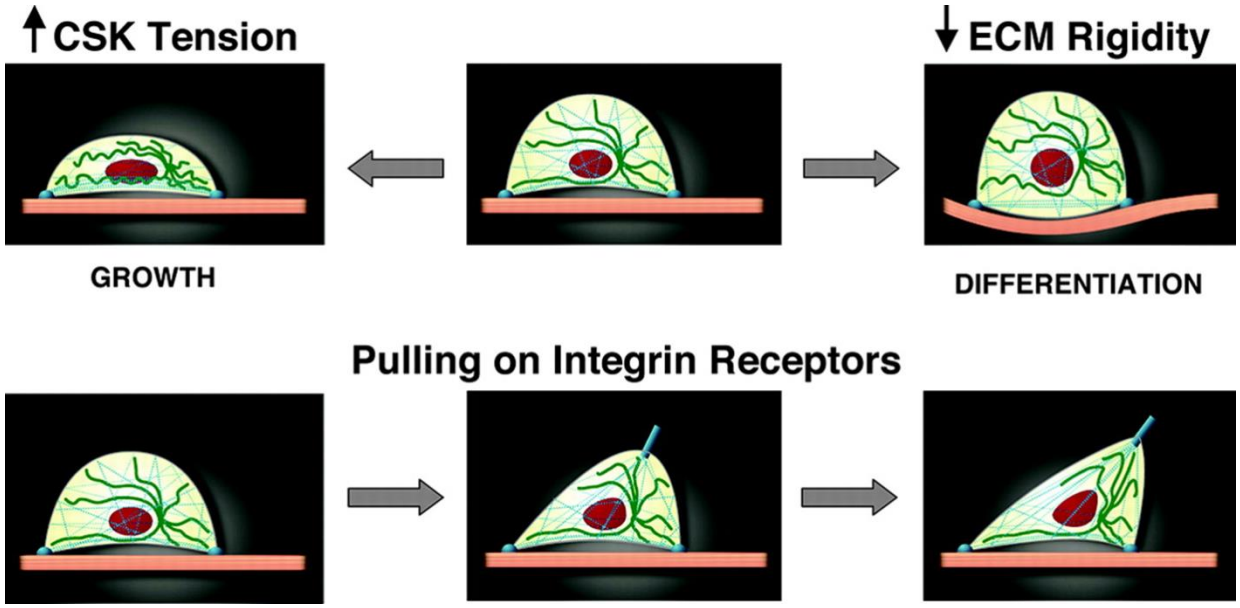

Figure 1.6: Integrated cell and cytoskeletal shape control through a complementary force balance between microfilaments, microtubules, and ECM. Top: Cell shape and the stability of the cytoskeleton depend on a mechanical force balance between microfilaments, microtubules and the ECM. In most anchorage-dependent cells, cell spreading on ECM is required for cell cycle progression and growth; abruptly increasing cytoskeletal tension in these spread cells results in cell flattening, increased bundling of actin filaments within basal stress fibers, and enhanced buckling of some microtubules (left). Decreasing ECM rigidity to the point where it can no longer bear cell traction forces results in force transfer to internal microtubules, which increases their buckling and bending, as well as stress fiber disassembly and cell rounding; in most cells, cell retraction switches off growth and turns on differentiation or apoptosis (right). Bottom: Diagram of a cell adherent to a rigid ECM through two basal focal adhesions (semicircles) showing the response of cytoskeletal microtubules (green) and microfilaments (dashed blue lines) when tensional forces are applied to integrins that form a focal adhesion on its apical cell surface

(cylinder). Pulling on integrin receptors results in coordinated structural rearrangements throughout the actin and microtubular cytoskeletons, as well as within the nucleus and basal focal adhesions. Pulling on other transmembrane receptors that do not mediate cell adhesion produces only a local membrane response (Ingber 2006).

1.3.2 Effect of neighboring cells on cell stiffness

As discussed in previous section, Integrin based mechanical dynamics have strong effects on cell behavior. In-vivo cells are connected also with neibhouring cells through e-cadherin junctions, which shares mechanical information and maintain proper tissue morphology and function. At cell–cell junctions, tension from actin and myosin in one cell can be transmitted to a neighboring cell (Gomez et al. 2011). These junctions serve a structural role, by maintaining cell integrity through cytoskeletal connections to other cells, as well as to the extracellular matrix.

Integrin based junctions are strong as compared to e-cadherins based cell-cell junctions, but yet the cadherins can mediate force-induced activation of Ca^{++} influx through mechanosensitive ion channels and associated actin assembly, and application of fluid shear stress to osteoblasts causes the cadherin-associated junctional protein, β-catenin, to translocate into the nucleus, where it activates gene transcription (Ingber 2006).

Many studies have highlighted cell-cell interactions in terms of adhesion and other chemo-physical properties, but only a few studies have been devoted to mechanistic nature of these interactions. Ivers *et al* studied interaction between MDA-MB-231 cells and non-cancerous epithelial cells (MDCK) in time lapse 3D configuration. They demonstrated that microenvironment has strong impact on the growth and dynamics of cancer cells by stressing the organ-specific affinity of cancer cells to host cells (Ivers et al. 2014). Songyu Hu *et al* by using optical tweezers pulling method categorized stroma- leukemia cell interactions as tightly adherent, loosely adherent and freely suspended (Hu et al. 2013). They also observed dynamic Wnt signaling pathways during cell-cell interactions by coupling optical tweezers to fluorescence microscopy (Gou et al. 2013). The effect on cell stiffness during cell-cell interactions was analyzed using AFM for normal, immortal, tumorigenic, and metastatic cells mimicking mammary epithelial cancer at four stages of aggressiveness (Guo et al. 2014), showing that microenvironment strongly affects normal cells (stiffer at the center and softer in isolated condition), but not metastatic and immortal cells and opposite effect was detected on tumorigenic cells. The reported body of evidences indicating that

the interaction between normal and neoplastic cell contributes to tumor growth (Kamińska et al. 2015). As invasive (metastatic) cancer cells don't express E-cadherins, their interaction with e-cadherins expressing cell will have different interaction mechanisms (Guo et al. 2014; Lee et al. 2012). Lee *et al* have shown that invasive cells are more mobile in the active interaction environment of non-tumorigenic epithelial cell line/normal as compared to non-invasive, tumoral cells. Invasive cells are softer and more sensitive to the physical forces and these forces are applied on the lateral surfaces of the cells (Lee et al. 2012).

Cell-cell interaction on soft substrate shows that some cells lose their shape sensitivity to substrate rigidity once they come into contact with other cells (Yeung et al. 2005). Cell–cell binding can overwrite cell-substrate induced signaling. In tissues, cellular-level mechanosensing, transduction and response processes can maintain the proper physical homeostasis, which is markedly altered in cancers (Suresh 2007; Yilmaz and Christofori 2010).

1.4 Optical tweezers in Biomechanics

The pioneering work by Ashkin et. al. on the trapping of micro- particles and their manipulation by radiation pressure (Ashkin 1970; Ashkin et al. 1986) led to the foundation of a new tool called optical tweezers or optical trapping (OT), which has found a multitude of applications in physics, chemistry and biology (**Figure 1.7**)(Grier 2003; Neuman and Block 2004; Ashok and Dholakia 2012). An important achievement for biology was the first demonstration that living micro-organisms (e.g. viruses, bacteria) could be manipulated by OT without being damaged (Ashkin and Dziedzic 1987).

Optical tweezers use an infrared laser and a microscope to trap an object and control its movements through photons (Neuman and Block 2004). When photons pass through an object, there is a change in their direction based upon the object's refractive index. The change in direction causes a change in momentum, resulting in a force on the object. When light is focused through a high numerical aperture lens, photonic forces can trap an object at the center spot of the laser beam (**Figure 1.7 c**).

For cell mechanical studies, a spherical dielectric bead is trapped which acts as handle to manipulate cells. Optical trap is characterized by the trap stiffness (*k)* and obeys Hooke's Law for small displacements (harmonic potential). Force which can be applied on the cell is then measured by the bead displacement *(x)* from the trap center. This displacement of the bead can be recorded

using video-based position detection, imaging or laser-based quadrant photodiode techniques (Neuman and Block 2004) . OT forces are in the range from 1 to 200 pN and trap stiffness is in the range 0.001–1 pN/nm.

Among the various properties of cell mechanics, viscoelasticity has been the most widely investigated using OT with varying experimental arrangements like, membrane tether pulling, cell stretching and indentation (Tavano et al. 2011; Dao et al. 2003; Zhang and Liu 2008; Rodriguez et al. 2013). The technique has continued to develop and evolve with time, and more suitable and stable algorithm are adopted, not only to broaden OT application and improve sensitivity, but also to match other biophysical techniques, like AFM. Therefore axial (vertical) optical traps are introduced having the same protocol of cell indentation as AFM (Yehoshua et al. 2015; Yousafzai et al. 2016; Coceano et al. 2016; Nawaz et al. 2012; Dy et al. 2013).

In the AFM techniques, the forces range from 10 to 10^3 pN with a cantilever stiffness larger than 10 pN/nm. However, there are some restrictions that limit its use in small force domain. The thermal noise of the cantilever in a liquid, which is of the order of tens of pN (Bodensiek et al. 2013), limits the minimum applied force. Furthermore, as an example, if the stiffness of the cantilever is 100 pN/nm (normally used in biological experiments), any small error in indentation of 1nm will induce a force of 100 pN, which is critical for many of the biological processes. To overcome these limitations, OT can be employed to characterize cell mechanics at small forces (<10 pN). OT, in general, impart forces in the range of 10^{-1} – 10^2 pN with a spring constant of 10^3 – 1 pN/nm, which makes OT ideal for low mechanical force regimes (Zhang and Liu 2008). The higher sensitivity of OT over AFM lies in the different kinds of probes through which they apply forces. In the case of OT, the probe is a micron size bead held tightly in a laser trap (Neuman and Block 2004), which is more sensitive than a mechanical cantilever (Zhang and Liu 2008).

OT versatility is highlighted by the wide range of applications which this technique has enabled: OT are now being used in the investigation of an increasing number of biochemical and biophysical processes, from the basic mechanical properties of cells (Tavano et al. 2011; Nawaz et al. 2012; Coceano et al. 2016; Yousafzai et al. 2016) to the multitude of molecular machines that drive the internal dynamics of the cell like DNA and proteins (Bustamante et al. 2003; Allemand et al. 2003), force generation by molecular motors (Block et al. 1990), individual RNA transcription (Wang et al. 1998), and protein unfolding/folding (Kellermayer et al. 1997) or binding/unbinding (Thoumine et al. 2000).

Lastly, it has been proposed that the optical trap may have detrimental effects on cells at higher laser power limits, due to the local heating from the high intensity of the laser, as well as photo-damage (Lim et al. 2006; Van Vliet et al. 2003; Hormeño and Arias -Gonzalez 2006). Therefore, we used an optimal laser power in our experiment to avoid any photo damage or changes in the mechanical properties of the cells.

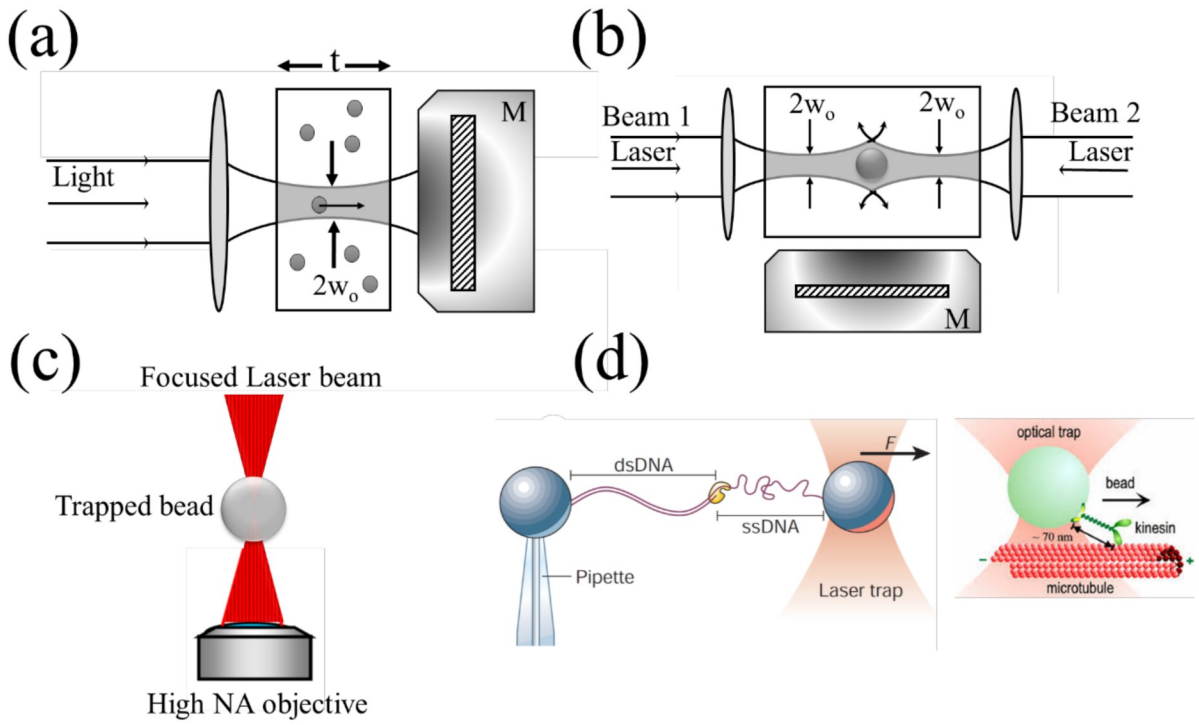

Figure 1.7: Evolution of optical tweezers. (a) The first observation made by Ashkin that particles are attracted toward and accelerated along the laser path. (b) The first optical trap made of two beams moving in opposite direction. (c) Single beam optical tweezers. Laser beam is focused by high numerical aperture (NA) lens, the beam traps dialectic bead which can be used as handle to apply forces. (d) OT used in DNA and motor protein study (adapted from (Ashkin 1970; Ashkin et al. 1986; Bustamante et al. 2003; Moffitt et al. 2008)).

1.5 Summary of the thesis

This thesis presents an attempt to study cancer cells from mechanical aspects, a rapidly expanding, yet still a nascent field of research that deals with the biomechanics and biophysics of cancer cells.

Chapter 1 sets the scene for mechanistic discussions. The formulation of the thesis begins with an introduction to some key observations on the mechanics of cancer cells. The architecture and load bearing components of cell i.e. Actin microfilaments, intermediate filaments and microtubule and their role in influencing cell mechanics, locomotion, proliferation, motility, differentiation and

neoplastic transformation are discussed. Cancer cell microenvironment and its importance in cell function and cancer progression and invasion in terms of cell-cell and cell-substrate interactions are highlighted. The chapter ends with the role of OT in biomechanics, which highlights some of its application limits and usefulness.

Chapter 2 introduces the materials and methods, used to study cell mechanical properties. Selection of breast cancer cells and the experimental mechanism of optical tweezers are described in detail. To mimic the physiological stiffness of the extracellular matrix, substrate modification with PDMS and collagen and preparation techniques are presented.

Chapter 3 discusses the experimental results in three sections.

Section 3.1 introduces the elastic properties of the three cell lines, and their comparison. The response of a cell to the applied OT force is showed to be almost elastic. We also presented regional variation is mechanical properties of the cells. We compare our result with AFM results and found the same kind of elastic modulus trend for all the three cell lines.

Section 3.2 is dedicated to the substrate dependent cell elasticity results. It is sowed that substrate stiffness has profound effect on cell elasticity. The cell senses the substrate rigidity and by changing the substrate rigidity the elasticity of the cell can be tailored.

Section 3.3 highlights the key role of cell-cell contact on the alterations of cell elasticity. These changes are dependent on the cell type and their level of aggressiveness.

Conclusions and Final Remarks conclude all the obtained results and highlight the future perspectives and directions.

Chapter 2
Materials and Methods

In order to study cell mechanical properties (cell elasticity/stiffness), two human breast cancer cell lines with different aggressiveness (MCF-7 (luminal breast cancer) and MDA-MB-231 (basal-like breast cancer)) and one normal immortalized breast cell line HBL-100 (normal, myoepithelial) were selected as a model. We also argued in the previous chapter that cell-microenvironment interactions are sensitive to mechanical forces in pN forces. Therefore, we employed OT setup to apply precisely calibrated pN forces and monitor the response of the cells in different microenvironmental conditions.

This chapter contains four sections. The first section describes the details of the three human breast cell lines chosen for the project: HBL-100, MCF-7 and MDA-MB-231. Second section is dedicated to the details of cell sample preparation. Third section specifies the procedures used for the coverslip coating with collagen and Polydimethylsiloxane (PDMS), used as soft substrates. The fourth section introduces Optical Tweezers (OT), discusses in detail the vertical indentation procedure and presents the procedure for elastic modulus calculation using Hertz model in two ways: fixed indentation range and fixed force range. At the end, details on the 3D bead position tracking and a comparison between the total indentation force and the vertical force are presented.

2.1 Breast Cancer Cell lines description

MDA-MB-231 is an estrogen receptor independent breast cancer epithelial cell line derived from the pleural effusion of a cancer patient. It is widely used for breast cancer biology studies; it belongs to the Basal cell-like (BCL) or “triple negative” phenotype. This subtype has been associated with aggressive behavior, poor clinical outcomes, lack of response to the usual endocrine therapies and shorter survivals when compared to other cancer subtypes. (Perou et al., 2000b; Foulkes et al., 2003; Sotiriou et al., 2002b). We used this cell type as a model of cancer cell with high aggressive behavior.

MCF-7 is an estrogen-receptor-dependent breast cancer epithelial cell line widely used for studies of breast cancer biology and hormone mechanism of action. The cell line was originally derived

at the Michigan Cancer Foundation from a malignant pleural effusion from a postmenopausal woman with metastatic breast cancer, who had been previously treated with radiation therapy and hormonal manipulation (Soule et al., 1973). The cells express receptors for a variety of hormones including estrogen, androgen, progesterone, glucocorticoids, insulin, epidermal growth factor, insulin like growth factor, prolactin, and thyroid hormone (Lippman et al., 1977). It belongs to Luminal A cell-like tumour subtype which is associated with good prognosis and a less aggressive behaviour, compared to the BLC group (Sotiriou et al., 2002b).

HBL-100 is an epithelial cell line developed and established in vitro, obtained from the milk of an apparently healthy 27-year-old Caucasian woman after three days from delivery (Gaffney et al., 1976;Gaffney EV., 1982). The milk donor was followed for several years with clinical and mammographic evaluations at regular intervals with no detectable breast lesion (Gaffney EV., 1982; Ziche and Gullino, 1982). However this cell line is referred to the breast in a particular situation, which is related to the production of milk. It is well known that gestation cycle induces a massive proliferation, but also the differentiation of epithelial subtypes of cells that are susceptible to neoplastic transformation (Wagner and Smith, 2005). The dual nature of the above mentioned myoepithelial cell line which for some experiments could parallel a normal cell, while for others is very similar to cancer cell is in line with other authors, who detected the amplification of c-myc even at low passages (Krief et al., 1989). At low number of passages (below P 35) HBL-100 showed to be non-tumorigenic, but they are able to form cancer in nude mice carcinomas at high number of passages. It has been shown that during the course of their progression toward neoplastic transformation, HBL-100 displayed an increasing capacity to induce angiogenesis and a loss of fibrin clot retraction activity, properties both associated with the malignant phenotype (Ziche and Gullino, 1982). HBL-100 cells, because of their myoepithelial differentiation, could represent a normal control for triple negative or basal breast cancers.

2.2 Cell sample preparation

Single cell studies: MDA-MB-231, MCF-7 and HBL-100 cell lines (ATCC numbers HTB-26, HTB-22, HTB-124 respectively) were cultured using low glucose Dulbecco's Modified Eagle Medium (DMEM) with L-glutamine (MDA-MB-231 and MCF-7) or Roswell Park Memorial Institute (RPMI) 1640 medium with L-glutamine (HBL-100), all supplemented with 10% (v/v) Fetal Calf Serum (FCS), 50 IU/ml of penicillin-streptomycin and 1mM gentamycin. Cell cultures

were maintained in 25 cm2 flasks at 37ºC in 5% CO2. Cell splitting was performed every 2-3 days, as soon as the cultures reached the confluence, using 1:10 diluted 0.05% trypsin-EDTA. The day before experiments, the cells were seeded overnight on 30 mm glass-bottom (OT) Petri dishes at a density of 10×104 cells/ml in 6ml (AFM) or 2 ml (OT and SSM) of medium. Before starting the experiment, the cells were washed three times in Phosphate Buffer Saline (PBS) and rinsed with medium prior to each measurement session. All reagents for cell culture were purchased by Gibco Lifetechnology, cell culture flasks and Petri dishes were purchased by Sigma-Aldrich.

2.3 Substrate coating procedure

2.3.1 Collagen coating:

To test the influence of the substrate stiffness on the elastic modulus of the cells, collagen-coated Petri dishes have been prepared and used for some experiments. Collagen is the main component of connective tissue and provides support for tissues. Type I collagen, the one that has been chosen for our experiments, has a herterotrimeric triple helical structure made up of two alpha-1(I) and one alpha-2(I) chains that twisted into elongated fibrils which are extremely strong. It has been proved to be useful as a substrate that promotes cell growth and proliferation (Hynda K. Kleinman et al., 1981). Under acidic conditions the protein is soluble, but it can be dried to form a thin layer of cell attachment. A concentrated solution of type I collagen was diluted with Acetic Acid 0.02N to a final concentration of 60µg/ml and has been distribute on a sterilized Petri dish to overlay the cover slip.

The glass has been kept in contact with the collagen solution for 2 hours under a biological laminar hood. The remaining solution was then removed and the Petri dish was washed twice with PBS. The Petri was air dried and put under UV light overnight for sterilization.

2.3.2 Polydimethylsiloxane (PDMS) coating:

The PDMS is a synthetic polymer belonging to the family of silicones, based on the relative composition of monomer and crosslinking agent, thin films o PDMS can be achieved having almost similar elastic modulus as that of physiological tissues (Chen et al. 2013). The PDMS is an optically transparent material, hydrophobic, inert and non-toxic. The hydrophobicity can be removed temporarily on the surface mediated oxidation plasma, converting the surface groups

from methylsilane to silano. This oxidized surfaces are then capable of binding proteins and support cell adhesions.

The protocol for PDMS coating on glass substrate was followed as (Chen et al. 2013)

- Addition of calculated amount of PDMS and crosslinker followed by vigorous mixing for few minutes.
- Degassing for at least 30 minutes to get a bubble free mixture.
- Coverslips cleaning using ethanol and followed by nitrogen drying.
- Spin coating of the mixture of PDMS on coverslip (rotation speed = 2500 rpm, rotation time = 20 seconds)
- Baking of PDMS coated substrates (85 ° C for at least 4 hours)
- Cooling and storage at room temperature up to a few weeks
- Plasma oxidation by using Plasma Cleaner (power = 50 W, time = 10 seconds, pO2 = 50 millibars) followed by immediate immersion of the substrates in sterile PBS.
- UV sterilization for 40-60 minutes.

The substrates of PDMS have proven transparent to infrared light and visible (Cai et al. 2008) allowing the correct operation of the optical tweezer systems and bright field microscopy for visualization of the sample.

In order to get a uniform thickness of the PDMS films, we optimized the parameters of time and speed of rotation of the spin coater to get thinness in the range from 40 to 48 μm. This thickness helps to avoid influence of glass substrate on cells. To obtain optimum parameters we performed several tests and deduced the required parameters form thickness vs time plots (**Figure 2.1**).

Due to the difference in composition of mixtures, and viscosity and hence the polymerization rate is different which leads to different spread on glass substrates. The substrates used for the experiments were fabricated at 2500 rpm for 30 seconds for mixtures 15: 1 and 35: 1, 3000 rpm for 30 seconds for the mixture 50: 1. These parameters allow to obtain thick substrates about 40 to 48 μm.

During the spin coating, the mixture of PDMS is distributed on the glass by means of centrifugal force, for this reason substrates tend to be slightly thicker at the edges.

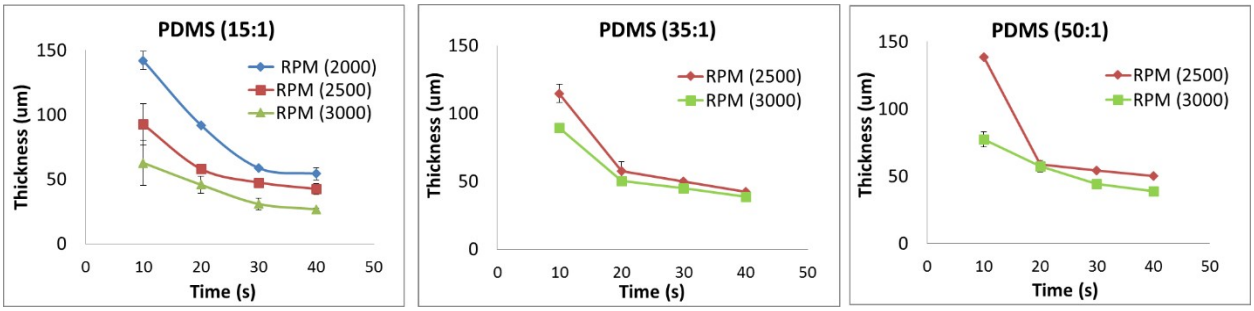

Figure 2.1: Optimization plots for PDMS spin coating. The plots were optimized for 40 to 48 µm of thickness with PDMS to crosslinker ratio as 15:1, 35:1 and 50 to 1 corresponds to 173kPa, 88kPa and 17kPa respectively.

2.4 Optical Trapping (OT)

A variety of biophysical methods such as microplate or optical stretchers, micropipette aspiration, magnetic twisting, atomic force microscopy (AFM) and optical tweezers (OT) are being used to study viscoelastic nature of cells, as reviewed in (Suresh 2007; Hoffman and Crocker 2009). However, in the past two decades, AFM and OT emerged as strong candidates to study cells cultured on substrates.

The majority of all optical trapping experiments are performed in a plane that is parallel to the microscope coverslip (Tavano et al. 2011). In this horizontal geometry, it is difficult to compare the quantitative results of optical trapping experiments with AFM indentation experiments because the experimental boundary conditions are very different. Therefore, we adopted a mechanism to probe the elasticity (stiffness) of cells, using the same vertical cell indentation scheme as AFM (Bodensiek et al. 2013; Yehoshua et al. 2015).

When analyzed with AFM in vertical indentation, the cells show elastic modulus values even three orders of magnitude higher than those obtained with OT. This highlights the fact that the cells are sensitive to the applied forces and the loading rates (measured in N/s) (Chiou et al. 2013) because of their viscoelastic, inhomogeneous and anisotropic nature. Therefore, for characterization of different cell lines it is important to complement AFM vertical indentation measurements by OT measurements following the same scheme (Yehoshua et al. 2015; Nawaz et al. 2012; Coceano et al. 2016). In AFM and OT techniques, where the cells are indented vertically for elasticity measurements, only the axial force is taken into account. We also introduce, the concept of total force which comprises both axial and lateral force components, and will be discussed in detailed in **section 2.2.5**.

2.4.1 Optical tweezers vertical indentation setup

A modular Thorlabs optical tweezers kit (www.thorlabs.com) with some modifications has been employed in this work. To achieve more stability and power we replaced the original laser trapping source (single mode laser diode, 975 nm, max 300 mW) by an IR laser (single mode Yb fiber laser YLM-5, 1064 nm, max 5W, IPG Photonics GmbH), as shown in **Figure 2.2**. The laser head has a built-in collimator providing a TEM00 laser beam with a diameter D=5 mm. After reflection by mirror M1 (which helps for alignment) the beam passes through a 2X beam expander, increasing its diameter to slightly overfill the entrance pupil of the microscope lens (Nikon 100X, NA 1.25 oil immersion, WD 0.3). This beam expander also helps to change the focus of the laser (trap position) to get a reasonable height from the coverslip and adjust relatively with respect to optical focus to better visualize the bead during cell-bead interaction as shown in figure 2.3. The laser beam is focused into the sample chamber by the microscope lens, where a silica microbead is trapped at the point of focus. A home-made temperature controlled holder (Tavano et al. 2011) is connected to the sample chamber (a Petri dish) to keep the cells at the physiological temperature, T= 37° C during the experiments. This is mounted on a nano-piezo cube, PS (Piezo Stage), (Thorlabs, NanoMax 3-axis flexure stage) allowing to control the sample position with 5 nm precision. A second microscope lens (Nikon 10X, NA 0.25, WD 7) collects the laser light scattered by the trapped bead. The scattered light interferes in the back focal plane (BFP) of the second lens. The interference pattern (IP) is imaged by lens L3 (f= 40 mm) onto the quadrant photo detector, QPD, (Thorlabs, PDQ80A, detector size 7.8mm) which senses the lateral and vertical displacement of the trapped bead, as indicated. When the bead is in the equilibrium position, the IP is centered on the QPD. A lateral displacement of the bead is indicated by an IP lateral displacement, while a vertical displacement is indicated by the change in size of the IP. The lateral and vertical differential signals (*ΔX, ΔY, ΔZ*) are obtained combining the signals from the quadrants 1-4 as follows:

$$\Delta X = [(1+4)-(2+3)]\,;\, \Delta Y = [(1+2)-(3+4)]\,;\, \Delta Z = [1+2+3+4] \qquad (1)$$

The differential signals are acquired through a digital acquisition card (DAQ – NI USB 2561) and a custom LabView (NI Student suit) code running on a PC. As the QPD has a large bandwidth (150 kHz), it can resolve the thermal movement of the bead in the trap very well, which is characterized by a maximum bandwidth of 1-2 kHz. The sample is illuminated by the light from a

LED through the second microscope lens. The sample is imaged by the first microscope lens and the tube lens (TL) on the sensor of a CMOS camera (Thorlabs, DCC 1240C).

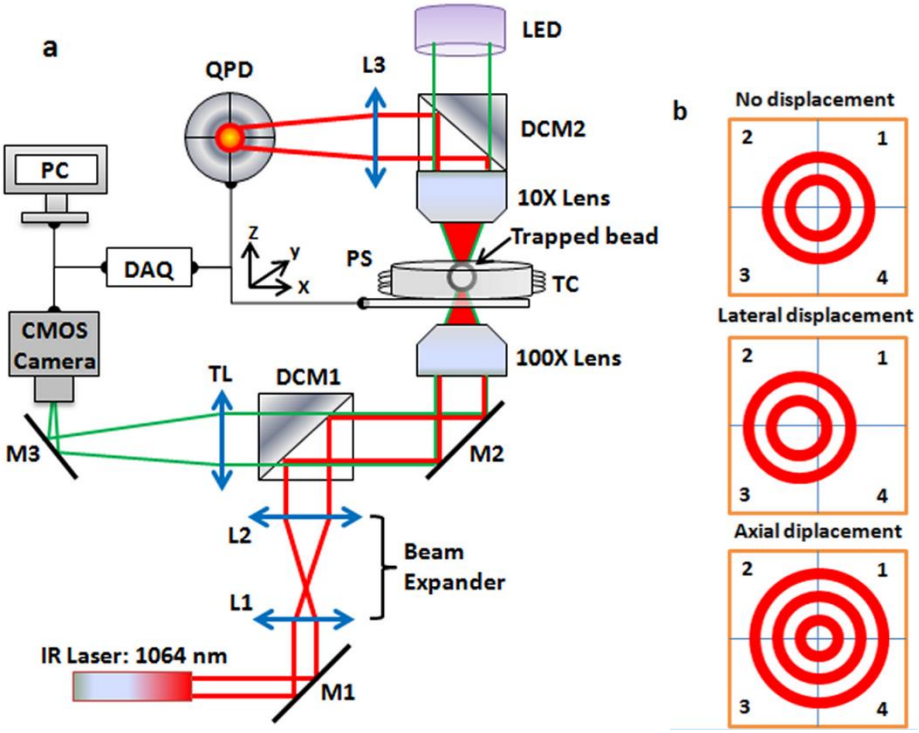

Figure 2.2: Optical tweezers setup for vertical cell indentation and force measurement. **(a)** Laser trapping beam path (red) and bright-field imaging path (green). PS: 3-axis nano-piezo stage; DAQ: digital analog acquisition card; TL: tube lens; L1-L3 convergent lenses; M1-M3: mirrors; DCM 1-2 dichroic mirrors, TC: temperature controlled holder **(b)** Interference pattern imaged on the QPD for: equilibrium position, lateral and axial displacements.

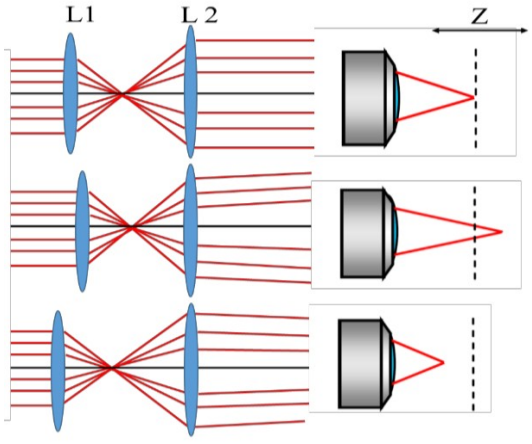

Figure 2.3: Changing the relative positions of the two lenses of the beam expender, one can increase or decrease the width of the beam as well as the trap location relative to the objective's focal plane (dotted line).

2.4.2 Calibration of optical trap

In order to use optical tweezers as a quantitative instrument for position and force measurements, the detection system must be calibrated. Silica bead of 3µm was used as a handle for measurements, to calculate and calibrate its stiffness (pN/nm) we take a time series position trace of the bead from QPD in terms of voltage as shown in **Figure 2.5**. The voltage trace acquired at 10 KHz for 5 seconds but only a section of 1 sec is shown, which is sufficient to calculate the stiffness. We used two calibration methods: the equipartition theorem and the power spectrum of thermal Brownian motion of a trapped object (power spectrum density - PSD). For the equipartition theorem we need to calculate sensitivity of our setup in terms of mV/nm in advance, while PSD doesn't require the sensitivity to be known. In the following, a detailed experimental procedure for calibration is presented.

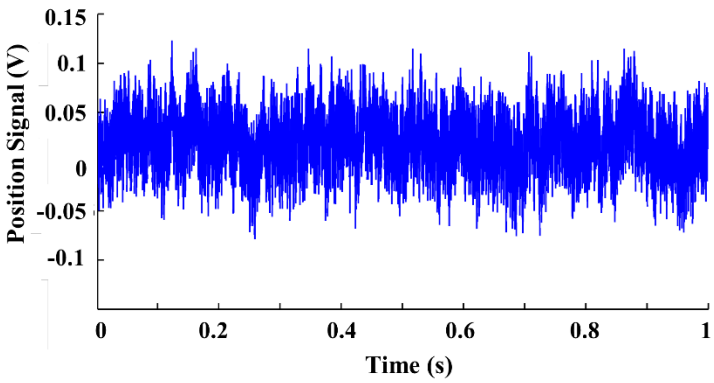

Figure 2.4: Trace of thermal Brownian motion of a trapped bead from the QPD in volts. The plot is a section (1 sec) of 5 sec trace sampled with 10 kHz.

2.4.2.1 OT setup sensitivity

To calibrate the position of the trapped bead and measure the linear range of the vertical optical trap we focused the trap onto a 3 µm diameter bead that was stuck to the coverslip. The stage was moved with a sinusoid of 1um, in order to sweep the trap through the stuck bead in the z-direction. The QPD signal in volts and the stage movement in µm was plotted to get the sensitivity of the setup **(Figure 2.4)**. The response was linear for ≈1 µm. From the slope we could obtain the detector sensitivity (0.5 mV/nm), which is necessary to convert voltage trace from QPD to position trace.

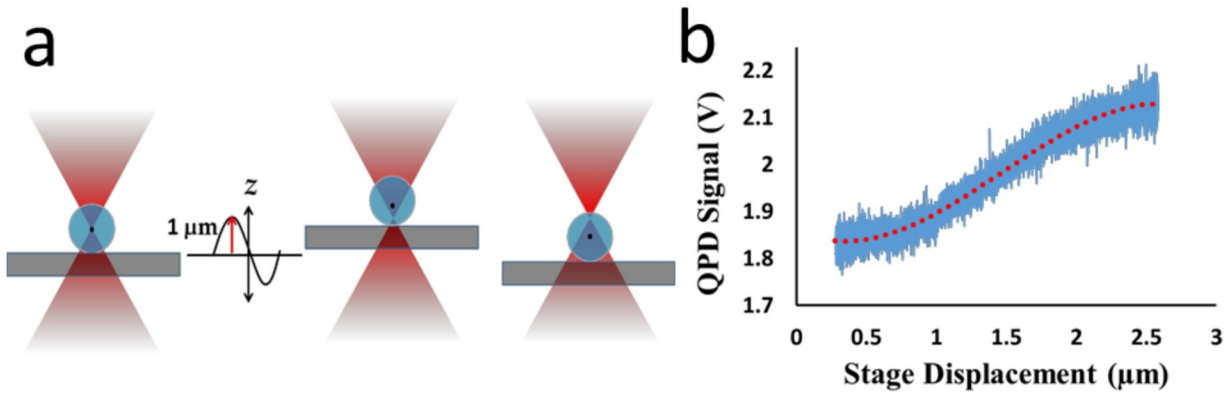

Figure 2. 5*:* (a) The stage with a stuck bead is moved sinusoidally with a 1um of amplitude, with trap focus is at the middle of the bead, and the QPD response is monitored. **(b)** By plotting the linear part of stage displacement and QPD voltage signal we get the QPD sensitivity in terms of V/µm. This plot also define the region of harmonic potential behavior of the trap.

2.4.2.2 Trap stiffness calculations

2.4.2.2.1 Equipartition theorem:

The equipartition theorem states that a molecule in thermal equilibrium has an average kinetic energy for each degree of freedom by

$$< E > = \frac{1}{2} K_B T \tag{2}$$

Assuming that the movement of the trapped bead is due to thermal fluctuations, we can set the kinetic energy to the potential energy of the trap.

$$\frac{1}{2} k < z^2 > = \frac{1}{2} K_B T \tag{3}$$

where $< \boldsymbol{z}^2 >$ is potition variance in the z direction. We can convert a voltage trace to a position trace using sensitivity and calculate the variance of the displacements $<\mathbf{z}^2>$, K_B is the Boltzmann constant and T is the temperature of the medium. Therefore, the stiffness of the trap is

$$k = K_B T / var(z) \tag{4}$$

2.4.2.2.2 Power spectrum density

The thermal motion of the bead was recorded from the QPD in volts and via a Fourier transformation converted into a power spectrum (**Figure 2.7**) and then fitted with a Lorentzian using **Equation 5**. The Brownian motion of the bead is constrained by the optical trap. However, at high frequencies (above the corner frequency f_c), the power spectral density of the trapped bead still represents that of the Brownian motion; at very short time-scales the bead does not feel the confinement of the trap. At frequencies below f_c, the spectral density is constant with a plateau I_0,

showing the confinement of the bead by the trap. A resonance peak is not visible in the spectrum because of the low Reynolds number of the bead; the trapped bead behaves like an overdamped oscillator (Bodensiek et al. 2013).

$$F(I, f, f_c) = \frac{I_0 f_c^2}{(f^2 + f_c^2)} \quad (5)$$

The estimating this corner frequency we can estimate the stiffness of the trap as

$$k = 2\pi\beta f_c \quad (6)$$

Where β is the hydrodynamic drag coefficient calculated as

$$\beta = 6\pi\eta R \quad (7)$$

Where η drag coefficient and R is the radius of the bead. The sensitivity is calculated by

$$s = \sqrt{\frac{\beta\pi^2 I_0 f_c^2}{K_B T}} \quad (8)$$

The power spectrum density method is fast as compared to the equipartition theorem method, as was stated earlier, the power spectrum density (PSD) doesn't needs prior estimation of the detector sensitivity. The method is also useful as a diagnostic tool for the trap stability.

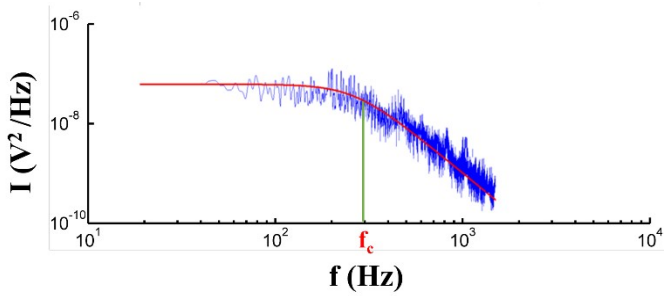

Figure 2. 6: Power spectrum density plot of bead's thermal motion in the trap. Fit with a Lorentzian (red line: using **Equation 5** for the corner frequency f_c.

2.4.3 Vertical Indentation Experimental Procedure

Cell indentation is observed by moving vertically the cell against the trapped bead, as shown in **Figure 2.7**. When contact is made, the bead will try to resist cell advancement, producing an indentation of the cell. As the stage displacement (*SD*) is known and bead displacement (*BD*) can be measured by BFP interferometry as previously shown, it is possible to measure the bead movement into the cells, i.e. the indentation, *Id*:

$$Id = SD - BD \quad (9)$$

The force, *F,* exerted by the cell on the bead during indentation is given by the linear relation:

$$\boldsymbol{F = k \times BD} \quad (10)$$

where *k* is the stiffness of the optical trap. This linear relation for the force is valid for a limited range of *BD* (± 1000 nm) (see **section 2.4.2.1**).

At the beginning of each single cell experiment, a bead is trapped and a cell is positioned slightly below it, preventing cell-bead contact. The Piezo stage (PS) is then vertically displaced with a sinusoid signal (amplitude A=1.14 µm, one period T= 5s) as shown in **Figure 2.7c**, and the vertical displacement of the bead in the trap is acquired at a 10 KHz sampling frequency (dark blue curve). During the first half of the period, the PS moves away from the bead, therefore the bead oscillates freely in the trap. This signal can be used to measure the stiffness of the trap *in situ*. It also confirm that there is no contact between the cell and the bead. As shown in **Figure 2.7c**, we chop up the signal for an interval, A of about 1 s to calculate the stiffness through the equipartition theorem with **Equation 4** (**section 2.4.2.2**). In this setup, the trap stiffness can be varied from 5 to 30 pN/µm using powers of the trapping laser, at the sample, from 8 to 50 mW. Stronger stiffness can be obtained by increasing the power of the laser, but this is limited by the need to avoid damaging the cell. It is to be noted, that cell damage is not restricted to the induced death of the cell but also to alteration of its properties (e.g. mechanical properties). To exert sufficient care in this regards we kept the trap stiffness at a constant value: k = 15 pN/µm (or 0.015 pN/nm), using a power of 24-26 mW of the trapping laser at the sample.

2.4.3.1 Contribution from Stoke's drag force:

By moving the stage towards the bead, we calculated the contribution of the Stoke's drag force to the total force. Using Stoke's equation

$$Fs = 3\pi\eta dv \qquad (11)$$

Where η viscosity of the media, d is is the diameter of the bead and v is the stage speed. The stage is moved with a speed of 1µm/sec, and selecting the viscosity of the medium as similar to water (0.069 Pa.s) at physiological temperature (37 ^{o}C). Inserting these values in **Equation 11**, we get the viscous drag force

$$Fs = 0.02 \text{ pN}$$

Since the viscous drag force is very low, we can safely neglect this contribution to the optical force.

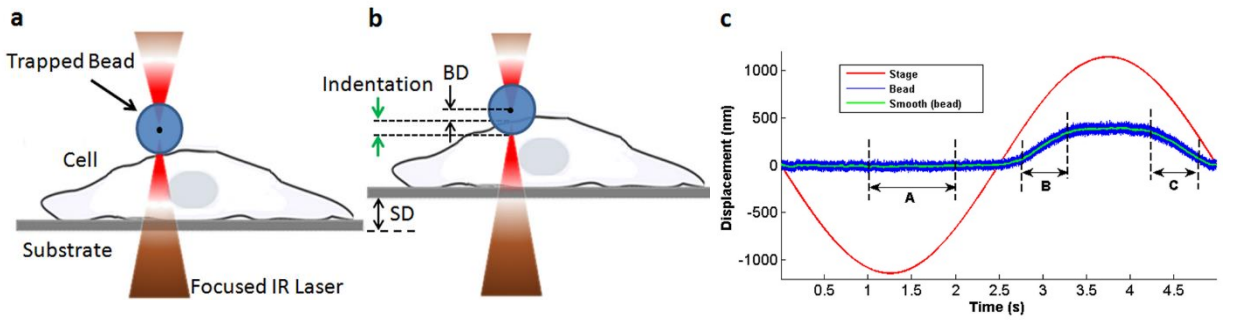

Figure 2.7: Schematic of the experimental procedure. **(a)** The cell is positioned below the trapped bead, **(b)** the stage is moved up by SD and the cell interacts with the bead displacing it by BD, while the bead indents the cell**. (c)** Stage and bead displacement due to cell-bead interaction. Stage displacement following a period of sinusoidal signal (T= 5s) is represented in red. Bead displacement sampled at 10 kHz is represented by the blue curve and the corresponding smoothed signal (over 500 sampling points) by the green one. Trap stiffness is calculated using the signal chopped from interval A, where the bead is freely oscillating in the trap. Indentation, B and retraction, C intervals defined in the linear regions of the second half of the sinusoid are used to calculate the elastic modulus

2.4.4 Elastic modulus calculation and data analysis

Data analysis and processing for elastic modulus calculations was performed using MATLAB ® (MathWorks®) code. Two schemes were used to calculate the elastic modulus from the experimental measured force - indentation curves: fixed indentation range and fixed force range, as it is described in the following sections.

2.4.4.1 Fixed indentation range

The interaction between the cell and bead is observed for the second half of the sinusoid shown in **Figure 2.7c**. When the cell comes into contact with the bead and begins to push it, bead displacement (*BD*) increases in the same direction as the piezo stage (PS) travel. However, the rate of *BD* rise is smaller than the rate of PS displacement. The difference between the two gives the cell indentation, *Id*. As shown in **Figure 2.7c**, there are two characteristic regions for cell-bead interaction: indentation, when the stage/cell moves toward the bead and retraction, when the cell moves back. To measure the elastic modulus, we choose shorter intervals B (indentation) and C (retraction), corresponding to the almost linear regions of the stage movement. To avoid ambiguities related to the contact point, the starting point of the indentation interval should correspond to a bead displacement $BD > 30$ nm. The same condition is maintained for the second

point of the retraction interval. Stage and bead displacements, indentation, the applied force and the selection of the indentation and retraction intervals are illustrated in **Figure 2.8a**.

The elastic modulus has been estimated by the use of the Hertz-model (Li et al. 2008). This model applies to homogeneous, semi-infinite elastic solid objects, but a living cell is clearly different from that type of object, being viscous as well as elastic, and inhomogeneous. In spite of this, the Hertz-model has been used to determine cell elasticity in most reported cell mechanics studies (Mierke 2014; Guz et al. 2014; Kirmizis and Logothetidis 2010; Laura Andolfi 2014; Li et al. 2008; Medalsy and Mu¨ller 2013; Nawaz et al. 2012; Dy et al. 2013; Coceano et al. 2016) and technical procedures of commercial AFM instruments (JPK; BRUKER). In our experiments, we consider the resulting elastic modulus as an *apparent* elastic modulus, to distinguish it from the rigorous formulation given by the Hertz-model. The *apparent* elastic modulus, E is given by (Nawaz et al. 2012):

$$E = [3\,(1 - v^2\,)\,/(4\,\sqrt{Id * R}\,)] * (F/Id) \qquad (12)$$

where, R is the bead radius, F the force, Id the indentation and v is the Poisson ratio. For our experiments we choose v= 0.4 (Nawaz et al. 2012).

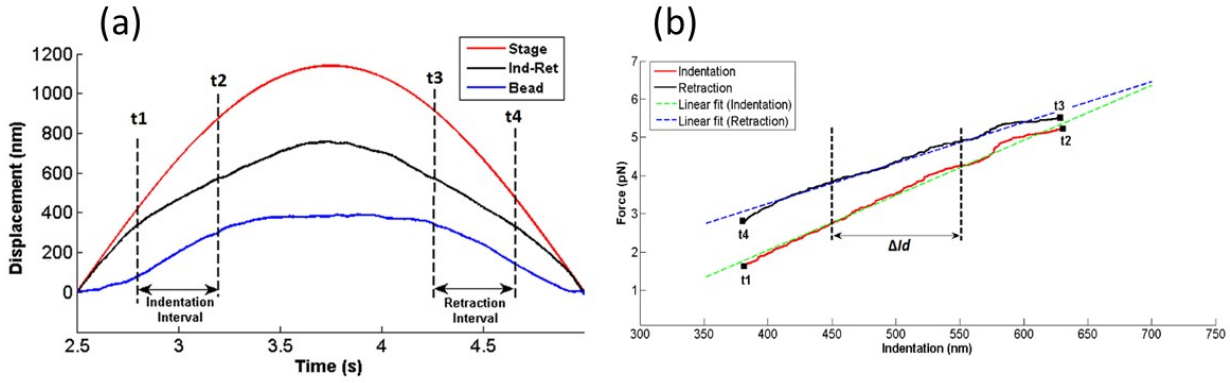

Figure 2. 8: (a) Indentation and retraction intervals. Stage displacement (red), measured bead displacement (blue), the calculated force (green), calculated indentation (black) for the second half of the sinusoid, when cell interacts with the bead. Indentation and retraction intervals are selected in the linear regions of the sinusoid. **(b)** Example of Force-Indentation plots taken for indentation and retraction intervals to calculate the slope S.

From the temporal sequences of *BD* and *Id* for the indentation and retraction intervals shown in **Figure 2.8a**, and using the force **Equation 10** we obtain the Force–indentation (*F-Id*) curves, shown in Figure 2.9b. As one can see from this figure, the curves are almost linear, indicating that

the behavior of the cell at low indentation forces is elastic. By linearly fitting the Force–indentation (*F-Id*) curve we obtain a linear Force-Indentation *(F_l-Id_l)* curve (Figure 2.7b) of which slope *S*, is: *$S= d(F_l)/d(Id_l)$*. Considering this linear fit, the elastic modulus in **Equation 12** can be approximated by:

$$E = [3\,(1 - v^2)\,/(4\sqrt{Id * R}\,)] * S \tag{13}$$

with the indentation *Id* remaining the only variable. Since the absolute value of the indentation depends on a series of experimental variables, such as the contact point, it is difficult to determine it properly. To avoid this problem we have adopted a practical criterion, based on the observation of the experimental data. From the temporal sequences of the indentation curves (**Figure 2.8a**) we observed an indentation, *Id* ≥ 200 nm, for all the cells analyzed in our study. The indentation and retraction intervals were therefore set to 200 nm. The starting point, t_1, of the indentation interval was always chosen to correspond to a bead displacement; *BD* > 30 nm, which confirms the cell-bead interaction event, while t_2 was chosen such that the interval [t_1, t_2] remained within the linear region of the stage displacement and the indentation amplitude, measured from t_1, was higher than 200 nm. The same criterion was used to establish the retraction interval. Following the above considerations, we calculated the elastic modulus considering the same indentation value, *Id* = 200 nm, for all the cells in our study. Introducing this value and the radius of the bead (*R*= 1.5 μm) in **Equation 13** we obtain a simple equation to calculate the apparent elastic modulus:

$$E = 1150 * S \tag{14}$$

where *S* is the slope of the linear force-indentation curve and the elastic modulus, *E* is expressed in Pa.

2.4.4.2 Fixed force range

The previous mechanism of elastic modulus calculations impose some boundary conditions on indentation by fixing indentation depth of 200 nm in order to get a slope of (F/Id) and linearize **Equation 14**. The procedure is technically correct but later we adopted a more appropriate one, which is generally used in AFM. : We fixed the force range by selecting a region defined by 0.15F_{max} to 0.75F_{max} in the force-indentation curve. Rearranging **Equation 13** we obtain

$$F = [\,4\sqrt{Id^3 * R}\,/(\,3\,(1 - v^2)\,)] * E \tag{15}$$

where E is to be determined using the $F(Id)$ curve. Since the equation above is not linear, we proceed with linearization in terms of Id:

$$F^{\frac{2}{3}} = E^{\frac{2}{3}} * C * Id \quad (16)$$

where C is a constant including all the other constants in formula (15). Fitting linearly the $F^{2/3}(Id)$ curve above, one can easily determine the value of the elastic modulus E.

From the bead displacement time series plot (**Figure 2.9a**), we select point **a** as a start of indentation till the highest point **b** on the curve, similarly the retraction region is from point **b** to **c**. The selection of points **a** and **c** are arbitrary but could be consider when the bead displacement curve takes-off or land on the base line. The force-indentation curve (**Figure 2.9b**) defines a range of forces going from the $0.15F_{max}$ to $0.75F_{max}$, to eliminate the effect of force saturation. This prevents the need to define the point of contact during cell-bead interaction and excludes the last part of the stage movement. The procedure is similar to that used for data processing in AFM experiments. If the automatically generated force range do not represent a linear range, a manual selection of force range is also possible. To calculate the elastic modulus we plot the linearized force – indentation values followed from **Equation 16**.

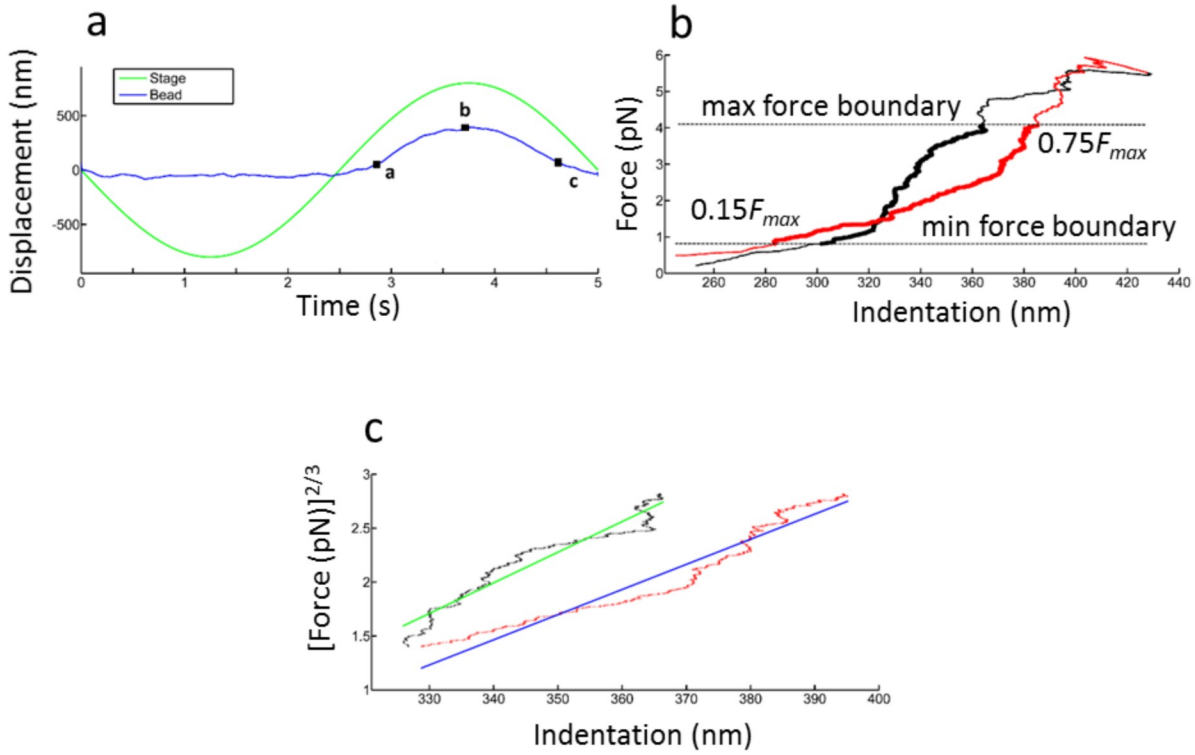

Figure 2.9: (a) Stage and bead displacement plot. The indentation range is from **a** to **b**, while the retraction region is **b** to **c**. **(b)** by selecting the maximum force on the force-indentation plot, a force region is automatically selected having range from $0.15F_{max}$ to $0.75F_{max}$. **(c)** Linearized force ($F^{2/3}$)-indentation (Id) curve plotted for **Equation 16**. (Indentation: black, retraction: red).

2.4.5 Total Force vs Axial Force

Our setup is capable to monitor the 3D movement of the bead (**Figure 2.10**) using QPD and hence the force components leading to calculate the total applied force on the cell. In most of the biophysical indentations experiments lateral components of the total force are generally ignored, and only vertical component is taken in to account. We used linearized Hertz model to calculate and compare the vertical and total indentations resulting from vertical and total forces, respectively. By tracking of the bead in the trap, we determine the trap stiffness, k, with its components $k = (k_x, k_y, k_z)$ (Neuman and Block 2004). Since the bead in the trap behaves as in a harmonic potential well, the force $F=(F_x, F_y, F_z)$ exerted on the bead is proportional to its displacement $BD= (BD_x, BD_y, BD_z)$:

$$F_x = k_x BD_x; \quad F_y = k_y BD_y; \quad F_z = k_z BD_z \tag{17}$$

We selected two breast cancer cell lines i.e. HBL-100 (transformed) and MDA-MB-231 (metastatic) and monitored the 3D tracking of the cell-bead interaction. We calculated and compared the elastic moduli resulting from the total and vertical forces, showing that the differences are important and the total force should be considered.

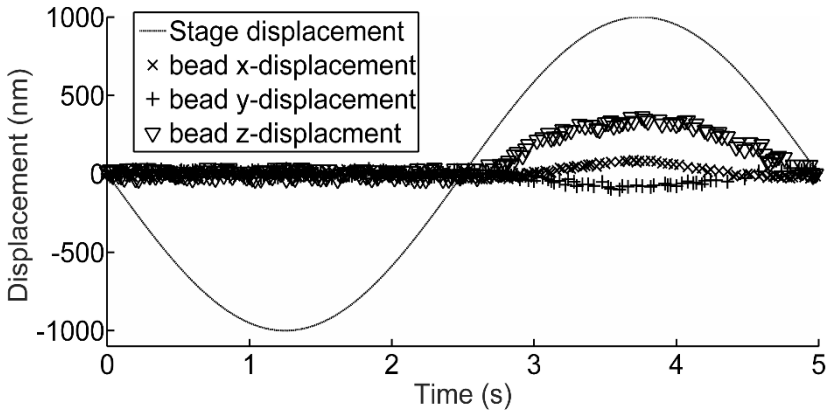

Figure 2.10: Displacement of the stage (cell) and of the microbead in the trap during the experiment. The sinusoidal movement of the stage make the microbead displacements: in x, y and z. The displacement of the bead in z begins to be significant and it is accompanied by smaller lateral displacements in x and y.

The trapped bead is positioned at a small distance above the cell (left image: **Figure 2.11**). The stage (and hence the cell) is moved vertically to intercept the bead (right image: **Figure 2.11**). The force exerted by the bead on the cell produces the cell indentation. This force is determined from the displacement of the bead (down image: **Figure 2.11**). If the bead displacement is vertical, the force has only one component, *F*(upper image: **Figure 2.11**) and the indentation, *Id*is only vertical. However due to the bead-cell interaction, the bead is displaced also laterally, which corresponds to lateral force components and hence the direction of the total force, *F* and of the indentation, *Id* are deviated from the vertical direction.

Following the same mechanism of cell indentation as discussed in **section 2.4.1**, we calculated the total force, *F* and its vertical component, F_z during the cell-bead interaction from the *BD* data, using **Equation 17**. As clear from **Figure 2.11**, due to the presence of lateral forces F_x and F_y, the total force *F* is different from the vertical component F_z.

We selected here, a model where the force has three components, but the situation may vary and the components and the angles may changes during experiments. Using the **Equation 17** we calculated the force components, the total force and its orientation. The force amplitude and

orientation are represented in **Figure 2.12 (a-b).** All the force components increase during the indentation and decrease during the retraction phase due to the cell-bead interaction. The total force F (○) is however larger than the vertical force F_z (▽), due to the lateral components F_x (x) and F_y (+). The orientation of the total force is not vertical and changes considerably, as indicated by the excursion of α and β **(Figure 2.12b).** The amplitude and direction fluctuations of the force indicate that the total force is a more adequate parameter than the vertical component only.

We considered both the indentation and the retraction interactions between the cell and bead interaction (see **Figure 2.12a**) and calculated the indentation elastic moduli E_i, E_i^z and retraction moduli E_r, E_r^z correspondingly from linearized force indentation curve (**Figure 2.12c**). We measured and compared the elastic moduli of 10 cells from MDA-MB 231 cell line and of 10 cells from HBL-100 cell line. The cells from each type of cell line were selected from two different cultures prepared in different days.

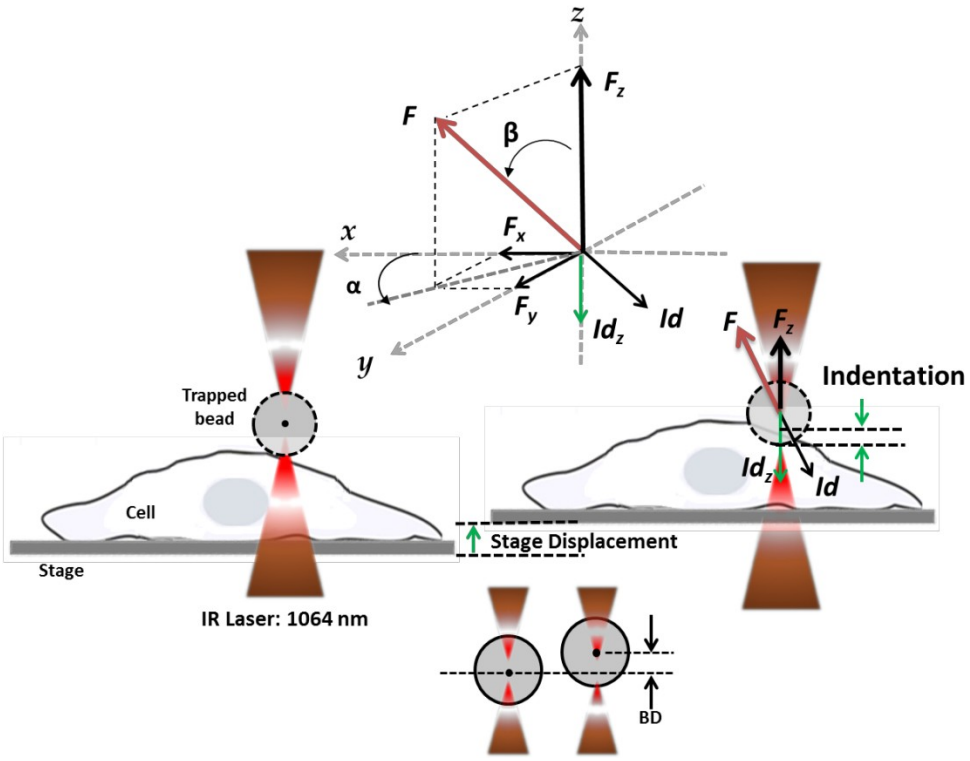

Figure 2.11: Experimental approach for calculating the force components (F_x, F_y, F_z) of the total force F during vertical indentation by optical tweezers. The vertical force is a component of the total force F.

As expected, the elastic moduli corresponding to the total force are bigger than those corresponding to the vertical force only, for both types of cells and for both indentation and retraction. The maximum difference between the mean value of the elastic modulus corresponding for total force and the elastic modulus corresponding to the vertical force is observed for HBL-100 cells. One can note from the standard deviation , the values are quite dispersed. This is typical for local measurements on live cells due to the variability of the cells: each cell is different from the other cells. Therefore, a larger number of cells should be considered when the investigation will be performed to provide relevant statistical analysis for cancer cell mechanics. Nevertheless, the values from **Figure 2.13** already indicate that HBL-100 cells are stiffer than MDA-MB-231 cells. This confirms the results of other studies reported in the literature (Wirtz et al. 2011), which show that basal aggressive cancer cells are softer than the non-neoplastic cells.

Figure 2.13 summarizes the results (mean-values). For HBL-100 cell line, the elastic modulus is higher for indentation than retraction by 17% when calculated from the total force. However no significant difference is observed for the axial force. For indentation, HBL-100 cells appear to be stiffer by 22% when the total force is considered than considering only the axial force component. For retraction the difference is smaller (7.8%). In case of MDA-MB-231 cells, the indentation and retraction values for elastic modulus for both total force and axial force are almost the same, indicating a clear elastic regime. Nevertheless for indentation, the elastic modulus calculated with the total force is 19 % higher than that obtained from the axial force. Similarly, the value is about 16% higher for the total force than the axial force during retraction.

The elastic modulus calculated for HBL-100 cells is larger than MDA-MB 231 cells for both indentation and retraction when estimated for total force and axial force. These measurements confirm that the metastatic MDA-MB-231 cells are softer as compared to HBL-100 cells. On the other hand, both cell types appear to be stiffer when probed with total force. This gives evidence of the contributions of lateral forces in cell bead interaction. These results suggest that considering the lateral forces provides a more accurate measurement of the effective elastic modulus, allowing a better analysis of the cell mechanics. All our measurements have been performed on the top of the cell, in a region above the nucleus. In a recently published paper (Coceano et al. 2016), using also AFM measurements at different positions of the cell, we have indicated this region as the most reliable to make a comparison between different cell lines in terms of cell elasticity. However, we expect that the differences between the cell elasticity results obtained when the total forces are

considered instead of the vertical forces, be considerably bigger in the transition regions between the nucleus and the leading edge. These aspects will be studied in detail in the next future by our group.

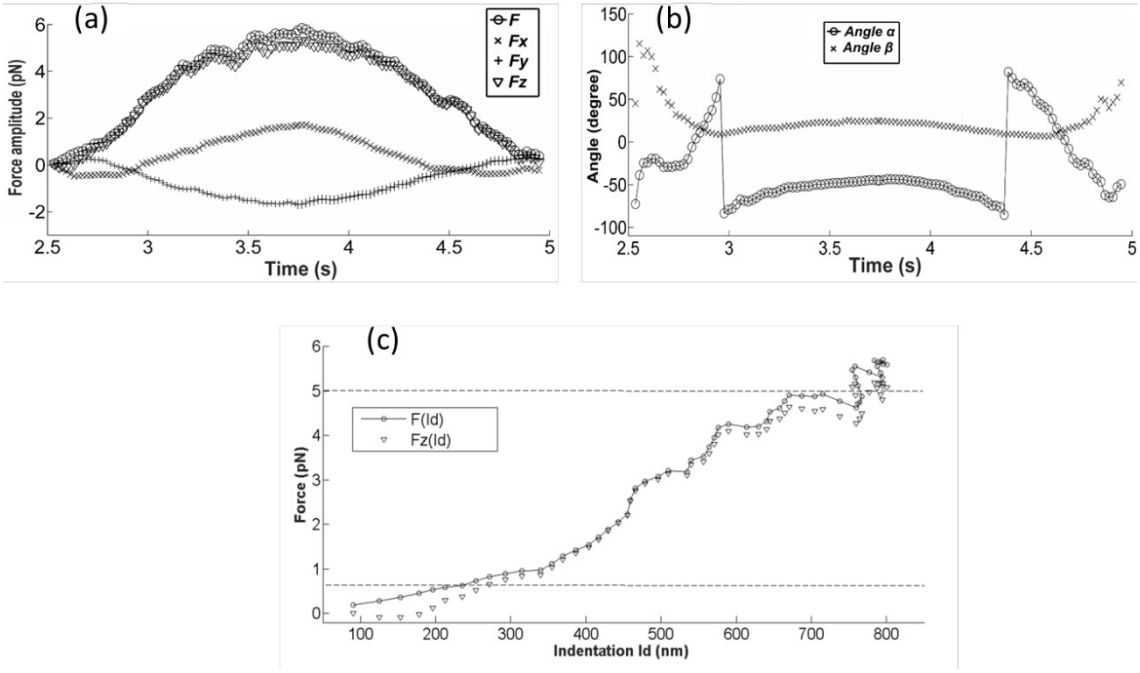

Figure 2.12: Force excursion vs time during the vertical indentation. **(a)** Total force F and force components: F_x, F_y and F_z; **(b)** The orientation of the total force F: angle α and angle β (angles defined in Figure 4). **(c)** Force-indentation curve for total force F, and the vertical force F_z. The dashed lines define the force range where the fit is applied.

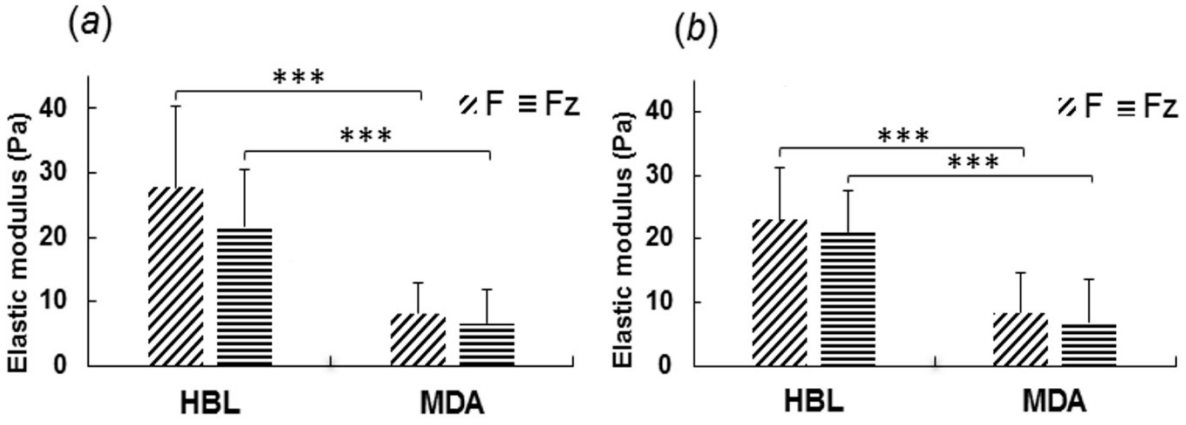

Figure 2.13: Elastic modulus values calculated for HBL-100 and MDA-MB-231 cells during **(a)** Indentation and **(b)** Retraction, using total force (F) and vertical force (F_z). (t-test: *** $p < 0.001$)

In summary, the elastic modulus found from total force are larger than its vertical component, suggesting that for more rigorous analysis, the total force should be considered rather than only the vertical force (Yousafzai et al. 2016).

Chapter 3
Results and Discussion

The elastic modulus values for the three cell lines, calculated using OT vertical indentation and hertz model, discussed in detail in the previous chapter, are summarized here.
This chapter is divided into three main sections. First, we presented the elastic modulus values for the three breast cell lines to differentiate them on the basis of their mechanical properties. Furthermore, the mechanical variation in different cellular subregions is presented in order to establish a consensus for cellular mechanical measurements. We also compared our results with AFM results to distinguish and map the cells on the basis of elasticity. Second, we summarize the results for mechanical properties measured on different complaint substrates like PDMS and collagen. Substrate stiffness has profound effect on the cell elasticity and morphology. Third, we relate alterations in cellular mechanical properties due to the cell-cell contacts. Neighboring cells change cell mechanical properties, making them stiffer or complaint depending of the nature and level of cell aggressiveness.

3.1 ELASTICITY OF CANCER CELLS AND ITS VARIATION IN CELLULAR REGIONS

Cancer is a multifactorial disease and there is a general consensus in identifying the hallmarks that better describe the onset and progression of the disease (Hanahan and Weinberg 2011). However, recently, attention has been focused on extra factors that characterize cancer: the mechanical changes that the tumor cells acquire and induce in the surrounding microenvironment (Mierke 2014; Hoffman and Crocker 2009; Plodinec et al. 2012). While this aspect is especially evident at the tissue invasion and metastasis stage, the overall change in the mechanical properties of a tissue starts much earlier, involving several physiological processes that, by altering the membrane and cytoskeleton structure, convert a malignant cell into a metastatic one (Plodinec et al. 2012; Costa 2004). It is known that cancer cells are softer and hence more deformable than non-tumour cells (Sugawara et al. 2008; Guck et al. 2005; Rother et al. 2014) and this eventually leads to their increased ability to infiltrate the tissues, spread from the primary tumour site and establish

secondary sites (Suresh 2007; Lekka et al. 2012). Metastasis is the most common cause of death in breast cancer patients. In females, breast cancer is the most frequent tumour (Jemal et al. 2011; Bacac and Stamenkovic 2008). Therefore a thorough characterization of the mechanical properties of breast cancer cells would be beneficial in the understanding of the underlying molecular events that lead to metastasis (Geiger and Peeper 2009; Cross et al. 2007) and could provide potential label-free markers based on mechanical measurements rather than molecular diagnostics (Cross et al. 2008).

3.1.1 Response of a cell to applied force

In general, cell's response to the applied force can be divided into two parts: a mechanical response (Janmey and Weitz 2004; Bausch and Kroy 2006; Gardel et al. 2006), consisting simply of the deformation of the cell's load-bearing structures, and then the biochemical signaling response, which potentially leads to force-induced phenotypic changes (Orr et al. 2006; Chien 2007; Wang et al. 1993). To understand the latter (biochemical response) one should have a complete knowledge of the mechanical response.

Here our focus is on the study of cell mechanical properties in different microenvironmental conditions.

Cells have complex microstructure and display viscoelastic behavior, having both elastic and viscous behavior (Nawaz et al. 2012). This behavior is ultimately due to the complicated, time-dependent response of interior architectural cytoskeletal components of the cells.

To understand how the cells respond to OT axial forces < 10 pN and loading rate of about 5 pN/s, we studied HBL-100 cells (n=26) on glass substrate. The bar plot in **Figure 3.1** suggests that the elastic modulus values for the indentation and retraction curves are almost identical (calculated from **Figure 3.2a**), indicating that the cell response to lower forces is almost entirely elastic (Coceano et al. 2016; Yousafzai et al. 2016).

In comparison, when HBL-100 cells were studied using AFM with force range of (1–2 nN) and indentation frequency of (0.25–0.5 kHz), there was a clear difference between the indentation and retraction curves as shown is in **Figure 3.2b**. This difference is an indicator of dissipation due to viscoelastic behavior of the cell at forces and loading rates specific to AFM (Coceano et al. 2016). For dissipative medium the retraction curve doesn't follow the same path of the indentation,

indicating that the cell respond to the indentation with a viscous component (Coceano et al. 2016) at high loading regime.

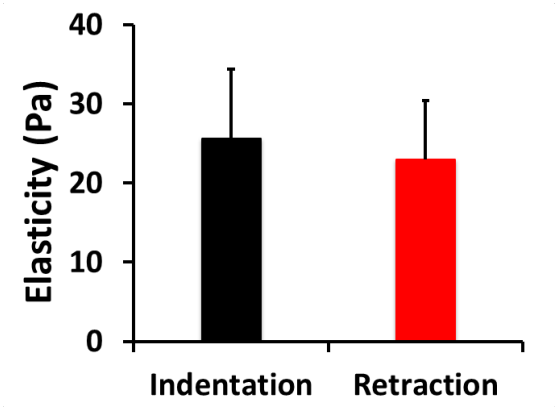

Figure 3.1: Mean elastic modulus values for HBL-100 cells for both indentation and retraction measured with OT. The two values lacks statistically significance, indicating elastic response of a cell to applied force. (N=26)

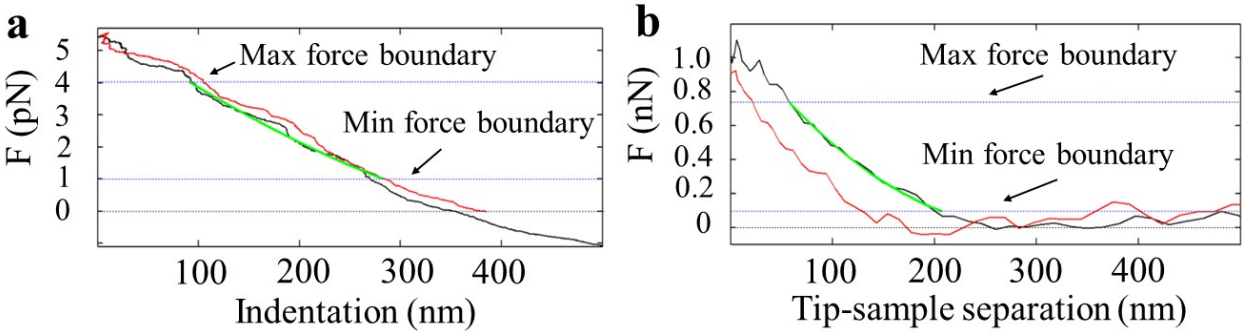

Figure 3. 2: Force-indentation curves on an HBL-100 cell using OTM **(a)** and AFM **(b).** The plots show the indentation (black), retraction (red) experimental traces and the fitted curves (green) used to calculate the elastic modulus. A Sneddon fit was used for AFM indentation **(a)** and a Hertz fit for OT **(b).** The fit is applied in a range of forces within min and max force boundaries. For OT the indentation and retraction curves are almost the same, indicating no loss of energy during indentation and retraction process, indicating an elastic behavior of the cell for low loading rates.

The viscous contribution could be explained by looking into the three components of the cytoskeleton (actin, microtubules, and intermediate filaments). These components have multiple interconnections and have a degree of spatial segregation. Normally, edges of cells are enriched in actin and comprises the cell cortex, whereas the microtubules and intermediate filaments are predominantly located in the middle of the cell, with the nucleus and an extensive network of lipid membranes comprising the endoplasmic reticulum and Golgi apparatus (Hoffman and Crocker 2009; Bao and Suresh 2003). In general , actin and intermediate filaments support the tensional forces (Wang et al. 2002) (Wang and Stamenović 2000), whereas compressive forces are supported by the microtubules and adhesions.

3.1.2 Elasticity and comparison of the three cell lines

To perform comparative studies on the basis of elasticity for the three cell line, we analyzed cells from different Petri dishes (about 6-10) and from different cell cultures, to have more representative information about the entire population. To have a better statistical population, more than 25 cells were selected for each cell line. The Elastic modulus values measured at the nuclear region in isolated condition are summarized in **Table 3.1** and **Figure 3.3**.

The results clearly show that the basal epithelial breast cancer cell line MDA-MB-231 has an elastic modulus lower than both luminal epithelial breast cancer cell line MCF-7 and the normal myoepithelial cell line HBl-100 cells, both for indentation and for retraction. The errors represent the standard deviations.

Table 3.1: Analysis of the Elastic modulus measured during indentation and retraction on the three different cell lines using OT. The table reports the values of the elastic modulus calculated as explained in the text and the number of independent measurements (n) from which the average value and the standard deviation (SD) were obtained.

		HBL-100 (n= 32)	MCF-7 (n= 30)	MDA-MB-231 (n= 25)
Elastic Modulus (Pa) ± SD	Indentation	**25.9** ±10.6	**31.6** ± 15.8	**12.6** ± 7.9
	Retraction	**23.4** ± 13.8	**31.2** ± 19.3	**12.6** ± 9.1

We compared the Elastic modulus values of the three cell lines obtained from OT with AFM results (**Figure 3.4**). Although the mean values of the elastic modulus measured by OT are always much lower than the ones obtained by AFM indentation, the cell lines comparison showed the same important result: the basal breast cancer cells, MDA-MB-231 has a significantly lower Elastic modulus than HBL-100 and MCF-7, regardless of the technique and loading rate applied for the measurement. The differences between the cell lines were calculated using the two tailed Mann–Whitney test.

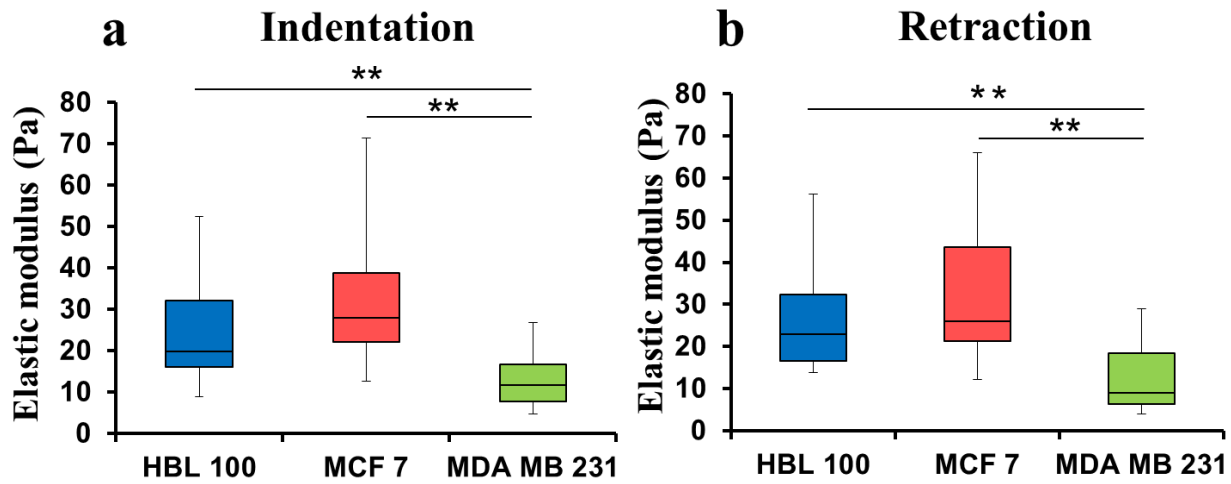

Figure 3.3: Box plot representation of the elastic modulus values for the three cell lines for (a) Indentation (b) Retraction. The Elastic modulus of MDA-MB-231 is significantly lower than the other two cell lines, the difference between HBL-100 and MCF-7 is not significant (*P: <0.05).

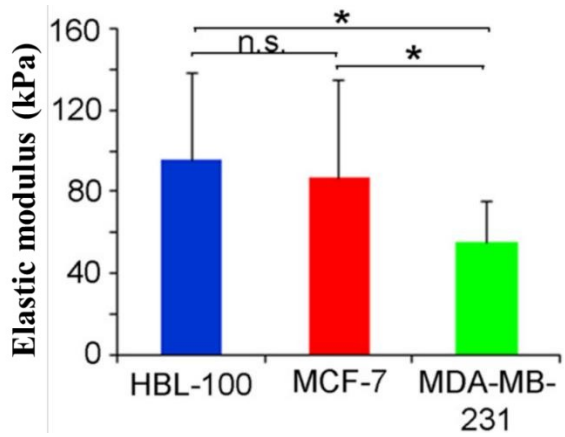

Figure 3.4: Bar plot representation Elastic modulus values for the three cell lines calculated with AFM. MDA-MB-231 has significantly lower (*P: <0.05) values than HBL-100 and MCF-7.

3.1.3 Cell regional variation in elasticity

Mechanical phenotyping of breast cancer cells using AFM and OT have shown that metastatic cells are softer as compared to the normal breast cells (Lee et al. 2012; Coceano et al. 2016) (Tavano et al. 2011). This comparison demands a robust strategy for comparative mechanical study of different types of cells. There are some studies (Guck et al. 2005; Guilak et al. 2000; Coceano et al. 2016) which show that the cell mechanical properties are in-homogenously distributed, with a nuclear region as the stiffer part. These observations indicate that for cell indentation experiments there should be a consensus among the regions of measurements on cells. Therefore to verify whether the elasticity is homogenously distributed across the cells when studied with OT and to

identify the most reliable measurement regions of the cells, we indented cells at three cellular locations: at the center above the nucleus (L1), out of cell nucleus (L2) and near the leading edge (L3), as shown in **Figure 3.5**. Each location was indented at least 2 times and the results were averaged for each location.

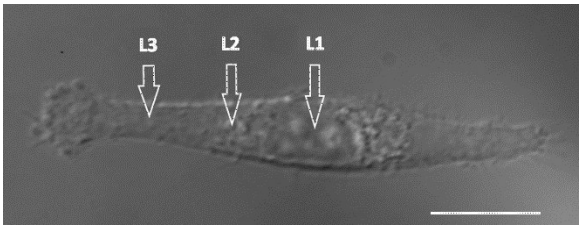

Figure 3.5: DIC image of a MDA-MB-231 cell and the indentation locations: L1 - above nucleus, L2 - intermediate position (cytoplasm) and L3 - near the leading edge. Scale bar 10 μm.

Biophysical approaches like AFM, optical stretching and micropipette aspiration which have been used to study viscoelastic properties of cellular sub regions (Lee et al. 2012; Guck et al. 2005; Guilak et al. 2000; Guo et al. 2014; Coceano et al. 2016). We used OT for the first time to study cell stiffness at three different cell locations. The results (**Figure 3.6, Table 3.2**) show a descending trend in elastic modulus from nuclear region towards the leading edge. All three cell lines exhibit higher stiffness at the center (L1) than the intermediate position (L2) yet having higher value than position L3 near the leading edge. The values at the three locations are statistically reliable and are in agreement with studies carried out by other groups using different biophysical methods (Guo et al. 2014; Guck et al. 2005; Guilak et al. 2000; Coceano et al. 2016).

Stiffness values for single cells indented at the center (L1) show that the most aggressive cells (MDA-MB-231) are softer as compared to HBL-100 and MCF-7. These values agree with the fact that metastatic cells are softer as compared to its non-invasive counter parts (Suresh 2007; Hoffman and Crocker 2009; Lee et al. 2012; Kristal-Muscal et al. 2013; Guo et al. 2014). The HBL-100 and MCF-7 cells are 2 fold stiffer than MDA-MB-231 in the nuclear region (L1) and can be used to differentiate cells on the basis of their aggressiveness level.

When comparing sub-regions, for HBL-100, stiffness at nuclear region is **25%** higher than cytoplasm and **47%** higher than the leading edge. MCF-7 stiffness decreases as **46%** and **59%** whereas for MDA-MB-231 it diminishes by **16%** and **47%** respectively for cytoplasm and leading edge. All the three cell lines have significantly different stiffness at the nuclear region and the leading edge, showing a larger contribution of the nucleus towards mechanical architecture (Guilak et al. 2000). **Figured 3.6** shows that HBL-100 and MCF-7 has the same elastic modulus at the leading edge as MDA-MB-231 at the center. Therefore, from these observation we can

conclude that for cells, to be mechanically characterized and differentiated, nuclear region is the most adequate for measurements. If the regional differences were disregarded then observations might be erroneous.

Table 3.2: Elastic modulus measurements (± standard error of the mean) for all three cell lines measured in isolated condition in three different cellular sub-regions. (L1, L2 and L3).

	Cell stiffness at cellular sub-regions in isolated condition					
	HBL-100		**MCF-7**		**MDA-MB-231**	
	E (Pa) ±SD	n	**E (Pa)** ±SD	n	**E (Pa)** ±SD	n
L1	**36** ± 11	10	**39** ± 8	10	**19** ± 9	14
L2	**27** ± 10		**21** ± 10		**16** ± 8	
L3	**19** ± 8		**16** ± 6		**10** ± 4	

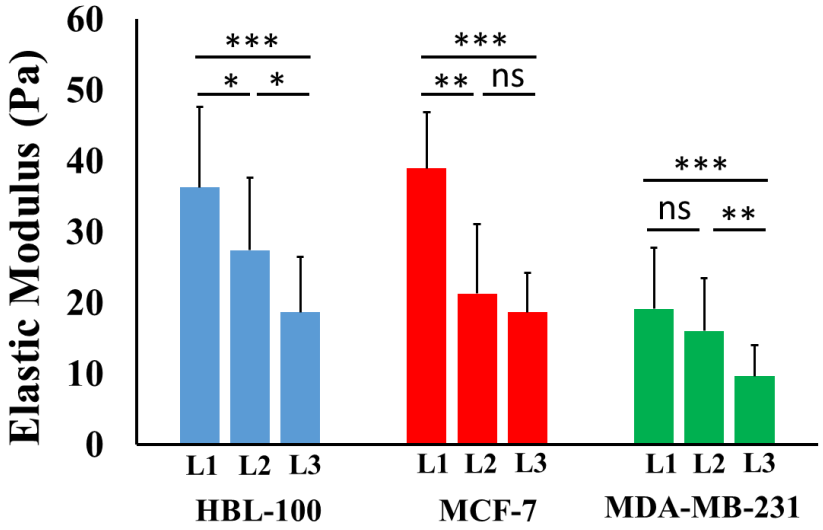

Figure 3.6: Elastic moduli for the analyzed cell lines indented at three cellular locations. All the three cell lines have descending character for stiffness, higher at the center and decreasing towards the leading edge. (t-test:*$p < 0.05$, **$p < 0.01$, ***$p < 0.001$).

When the same cell lines were mapped with AFM, the same elasticity trend was observed as shown in **Figure 3.7**. By comparing the two data sets it is clear that even a low loading rate has the outcome for elasticity and can be used as complimentary technique to AFM.

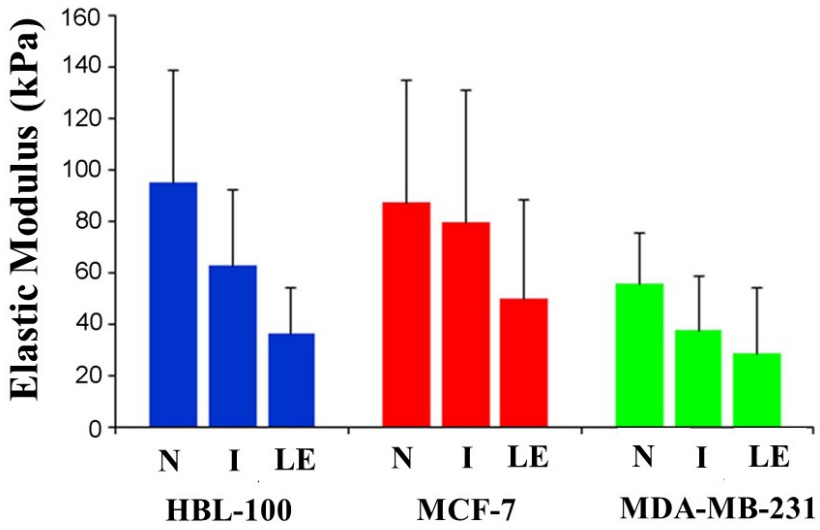

Figure 3.7: Elastic modulus values measure with AFM. The elasticity decreases with the distance from the nucleus. N: nuclear area, I: intermediate, and LE: leading edge.

3.1.4 Conclusion

Here we applied OT vertical indentation technique to distinguish breast cell lines on the basis of their elasticity which serve as an indicator of cell aggressions. As a first observation, we found that cells response is elastic for low loading rates and low forces. For comparative observations, we found that metastatic cells (MDA-MB-231) are softer as compared to HBL-100 and MCF-7. Further, we realized that cell's response is different at different cellular regions and this might nullify our claim. Therefore to have a consensus for mechanical characterization of cells, we studied regional mechanical variation in cells and show that all the three cell lines exhibit descending trend in elasticity from center towards the leading edge. The results show that nuclear region is the stiffer part and can be used for mechanical characterization of cells. We compared our results with AFM measurements (with high loading rates) and found an agreement in results. OT rules out the contributions of viscous forces typical of AFM and measure the elastic behavior of the cells. Also, the regional mechanical variations were found to be the same as AFM. Our results show that measurements region on the cell influences results: stiffness decreases from the center towards the periphery (leading edge).

3.2 EFFECT OF SUBSTRATE STIFFNESS ON CELL ELASTICITY

In vivo, epithelial breast cells are mechanically anchored on extra-cellular matrix (ECM), like collagen, fibronectin etc, and they are constantly in mechanical force balance (DuFort et al. 2011; Kumar et al. 2006; Wang et al. 2001; Ingber 2003; Hu et al. 2004). When an imbalance occurs (mechanical and biological) these cells becomes cancerous, their mechanical anchorage properties changes and they become motile and metastasize (Kobayashi and Sokabe 2010). These metastic cells have much different mechanical properties from the normal cell (Suresh 2007). The mechanism how these cells actually migrate out of primary tumors and invade into neighboring tissue (how they intravasate and extravasate) is still elusive (Bacac and Stamenkovic 2008). These cells are generally not viable when suspended in a fluid and are therefore said to be anchorage dependent. Normally, in lab based experiments, they are studied on Glass substrates having stiffness in range of GPa. However, cells feels the stiffness of the underlying substrates and change their stiffness accordingly (Solon et al. 2007) (Engler et al. 2006). Therefore, different attempts have been made change the stiffness of the underlying substrate and mimic the same stiff as that of tissues and ECM (Khademhosseini 2008; Pelham and Wang 1997).

Here in this Section we modified the glass coverslips with polydimethylsiloxane (PDMS) and collagen and studied the elastic properties of these cells. The elastic properties of cell on these substrates are indicator of cell's aggressiveness.

3.2.1 Polydimethylsiloxane (PDMS) as soft substrate

To investigate whether cell elasticity is affected by the stiffness of the substrate to which they adhere, we studied cell's elastic modulus on polydimethylsiloxane (PDMS). PDMS has been extensively used as a material to study cell behavior because of its biocompatibility and the tunable mechanical properties that cover a wide range of biological tissue stiffnesses (Yim et al. 2005; Murrell et al. 2011; Trappmann et al. 2012). We prepared three PDMS substrates with bulk stiffnesses of 173 kPa, 88 kPa an 17 kPa by varying the base:crosslinker ratio as 15:1, 35:1and 50:1 respectively (Chen et al. 2013). The height of the PDMS film was maintained at 40-50 µm such that the cells don't feel the glass rigidity (**Figure 3.8**).

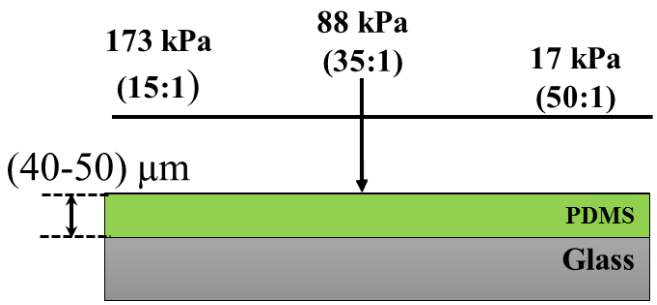

Figure 3.8: Glass coverslips are coated with PDMS to get complaint substrates. The ration of polymer to crosslinker was used as 15:1, 35:1and 50:1 to get stiffness of 173 kPa, 88 kPa and 17 kPa respectively. The height of the film was 40 µm - 50 µm to avoid glass rigidity effects on cells.

Twenty cells from each substrate were analyzed from different sets of cultures. Measurements were performed for all cells in their central region, above the nucleus. Results are summarized in **Table 3.3.** From the bar plot (**Figure 3.9)**, it is evident that the elasticity of HBL-100 and MCF-7 cells decreases with the softness of the substrates, while MDA-MB-231 shows an increase in stiffness. **Figure 3.10** shows the bright field images of the morphologies of the three cell lines on glass and PDMS substrates. All the three cell lines show viability and biocompatibility with PDMS.

HBL-100 on a glass substrate spreads more as compared to PDMS where it adopts a compact morphology. HBL-100 cells are softer on PDMS where they adopt a compact morphology. HBL-100 shows a decreasing trend in elasticity with the decrease of substrate stiffness.

MCF-7 cells also show a decrease in elasticity with softness of the substrate. The morphology of the cells show a compact structure. There is no statistical difference in elasticity between glass and PDMS for 173 kPa and 88 kPa, which indicates that for this stiffness range MCF-7 does not feel the underlying substrate stiffness. There might be two possibilities, since the structure is compact on PDMS but the spread area is the same as on glass which give the same elasticity. Secondly, there may be some critical value of stiffness for MCF-7 cells to respond to the substrate stiffness.

Contrary to HBL-100 and MCF-7, MDA-MB-231shows polarization on soft substrates (**Figure 3.9f)**. As MDA-MB-231 cells are metastatic and motile, their response is different to compliant substrates. MDA-MB-231 shows increase is stiffness with the softness of the substrate as show in **Figure 3.10**. The elasticity plot of MDA-MB-231 indicates that there is an increase in stiffness for glass to 173kpa, and then a decrease towards 17kPa. We have no clear idea but there might be

some critical threshold stiffness of PDMS to which MDA-MB-231 cells are sensitive and can be identified if the stiffness range is analyzed with small steps.

Table 3.3: Elastic modulus measurements (± standard error of the mean) for all three cell lines measured in isolated condition on three types of PDMS substrates. (15:1, 35:1, 50:1).

	HBL-100		MCF-7		MDA-MB-231	
Type of Substrate	**E (Pa) ±SD**	**n**	**E (Pa) ±SD**	**n**	**E (Pa) ±SD**	**n**
Bare Glass (70 GPa)	**36.7** ± 12	20	**31.3** ±7	20	**18** ±8	20
PDMS 15:1 (173 kPa)	**32.7** ± 18.3		**30** ± 8		**34.8** ± 17	
PDMS 35:1 (88 kPa)	**27.2** ± 9		**38** ± 8		**33** ± 6	
PDMS 50:1 (17 kPa)	**25.6** ±11.5		**25** ± 12		**22** ±14	

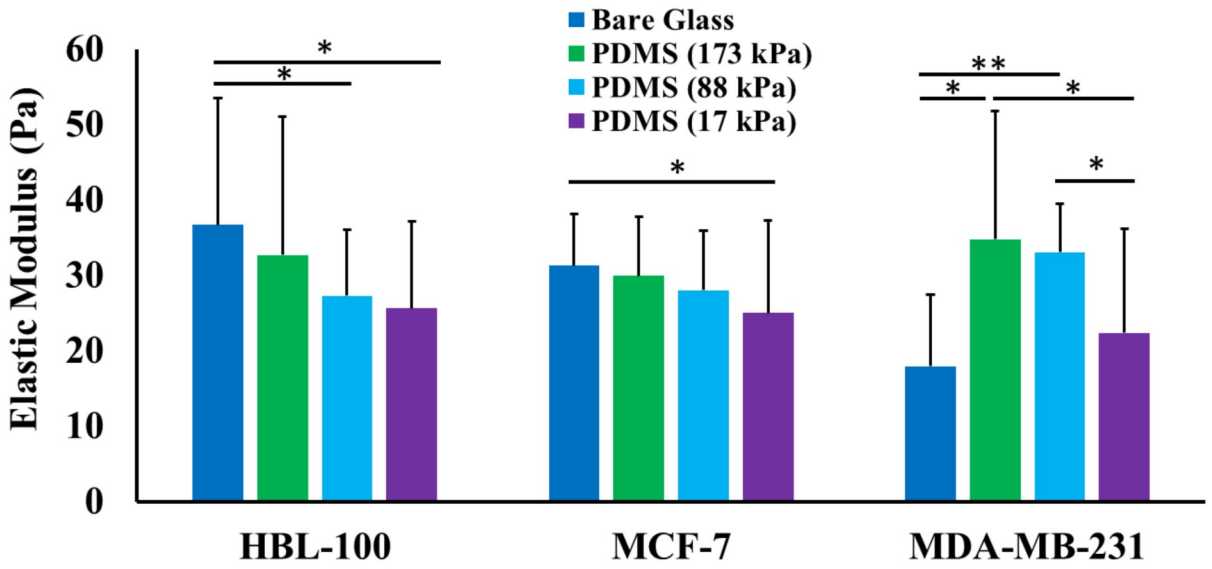

Figure 3. 9: Elastic moduli for the three cell lines plated on three different PDMS substrates (173kPA, 88kP, 17 kPa). HBL-100 and MCF-7 shown a descending trend in elasticity with a decreasing PDMs stiffness. While MDA-MB-231 has increased stiffness. (T-test:*$p < 0.05$, ***$p < 0.001$).

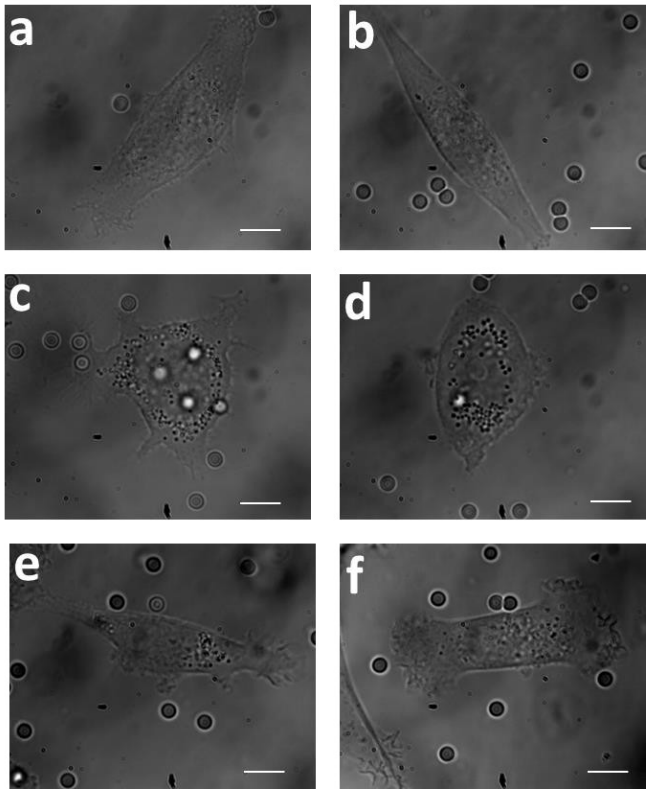

Figure 3.10: Bright field images show morphology of HBL-100 cells on glass **(a)** and PDMS **(b)**; MCF-7 on glass **(c)** and PDMS **(d)**; and MDA-MB-231on glass **(e)** and PDMS **(f)** substrates. HBL-100 and MCF-7 show compact structures on PDMS while MDA-MB-231 shows polarization at two ends. (Scale bar 10µm)

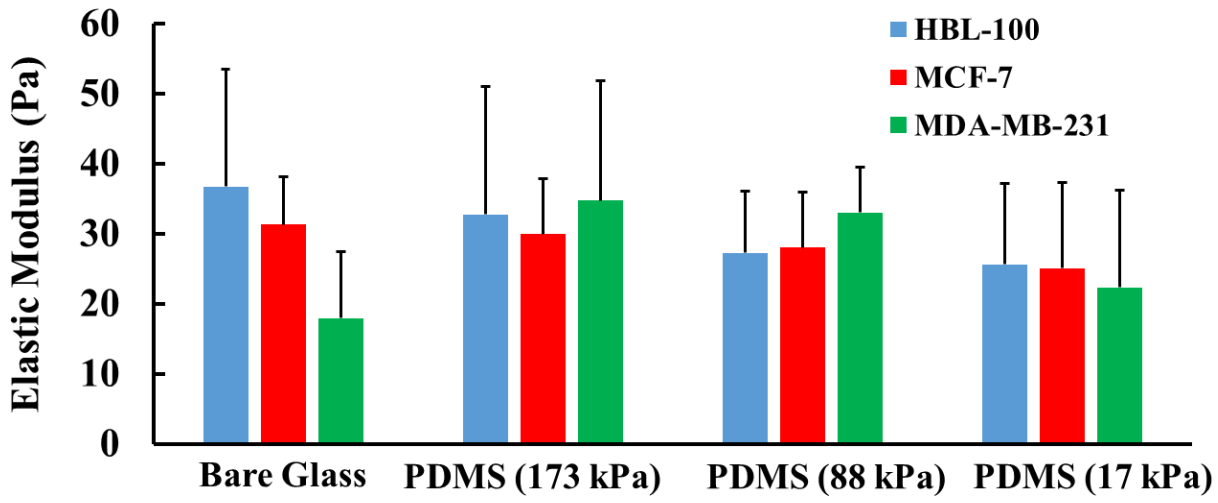

Figure 3.11: Comparative representation of elastic modulus values for the three cell lines plated on glass and three different PDMS substrates (173kPA, 88kP, 17kPa).

Figure 3.11 indicates that on glass substrate we can clearly distinguish MDA-MB-231 from other cell lines by stiffness, while on PDMS we cannot because the stiffness values are comparable for

all the cell lines, without a significant difference between them. However, the increase of stiffness for MDA-MB-231 for softer substrate can be used together with the measurements performed on bare glass to confirm cell elasticity as a marker to differentiate and characterize metastatic cells.

3.2.1.1 Discussion

Mechanical interaction of cell with soft gel for the determination of metastatic potential (MP) of cancer cells and to identify and predict the metastatic target-site in the body is one of the emerging tools in cancer research. Cells constantly interact mechanically with their underlying matrix (substrate) through integrin based focal adhesions (Schoen et al. 2013; Mierke 2014). Mechanical properties of matrix are crucial, as they may have a role in cancer initiation, promotion or they may cause the cancer to revert back (Bissell and Hines 2011; Ingber 2008). Some studies show that by tailoring the matrix stiffness, cancer cell fate may change to normal ones (Bissell and Hines 2011; Ingber 2008). Evidence indicates that in cancer microenvironment, ECM becomes stiffer as compared to its normal state, but cells behave softer (Katira et al. 2013) and exhibits increased acto-myosin cortex contractility (Kristal-Muscal et al. 2013). Kristal et al show that that invasive, metastatic cells apply normal forces and indent the impenetrable, soft gels utilizing their cytoskeleton, and also apply strong lateral (traction) forces. In contrast, benign cells that remain rounded on the gel, do not indent, and apply small normal and traction forces (Kristal-Muscal et al. 2013). Here, our results shows that HBL-100 and MCF-7 cells are getting softer with the softness of the substrate, while the metastatic cells, MDA-MB-231, exhibit an increase in elasticity with the decrease in substrate stiffness. This increase in stiffness may be attributed to increase in acto-myosin activity during cell motility and force generation. However, not only substrate stiffness plays decisive role for controlling cell adhesion and hence cell stiffness but also a specific mechanical anchorage of adhesion molecules like collagen, fibronectin (Trappmann et al. 2012) . Our results show that even without anchorage molecules the cell lines adhere to PDMS substrates and adapt their morphology closely related to their physical state i.e. either tumorigenic or metastatic.

3.2.2 Collagen as soft substrate

Collagen, a major constituent of the extra cellular matrix (ECM) *in vivo*, has been used as a soft substrate for cells to study substrate influence on the mechanical behavior of cells *in vitro* (Yang and Nandi 1983; Plant et al. 2009; Holle et al. 2015*)*. We used type I collagen, normally found in

bones, tendon and skin. The superiority of the collagen substrate, whether used as surface or as matrix culture, over plastic and glass may lies in its ability to allow cells to produce a basement membrane (Yang et al. 1981)

We used HBL-100 cell line cultured on two different substrates: bare glass coverslip and collagen coated coverslip. Bare glass represents the stiffer substrate, while collagen-coated glass represents the less stiff substrate (Wen and Janmey 2013; Khademhosseini 2008). Twenty-six cells from each substrate were analyzed from different sets of cultures. Measurements were performed for all cells in their central region, above the nucleus. Results are summarized in **Table 3.4**. HBL-100 cells cultured on glass have an elastic modulus higher than the one of the cells grown on collagen-I coated substrate, both for indentation and for retraction. For the glass (stiffer) substrate, the elastic modulus measured during indentation was 27% higher than that obtained for the more compliant collagen substrate. For retraction, the difference between glass and collagen-coated substrates was even larger, notably 43 %. For both substrates, the elastic modulus measured for indentation was smaller than the one measured for retraction (by 11.5 % for glass substrates and 31.6 % for collagen-coated substrates).

Our results show that cell elasticity correlates with the substrate stiffness; HBL-100 cell elasticity increases when cells are cultured on stiffer substrate.

Table 3.4: Elastic modulus values for indentation and retraction of HBL-100 cells cultured on bare and collagen-coated glass substrate. The table reports the values of the elastic modulus calculated as explained in the text and the number of independent measurements (n) from which the means and the standard deviation (SD) were obtained.

		Bare Glass	Collagen-coated Glass	n
Elastic Modulus (Pa) ± SD	**Indentation**	**26** ± 9	**19** ± 7	26
	Retraction	**23** ± 10	**13** ± 7	26

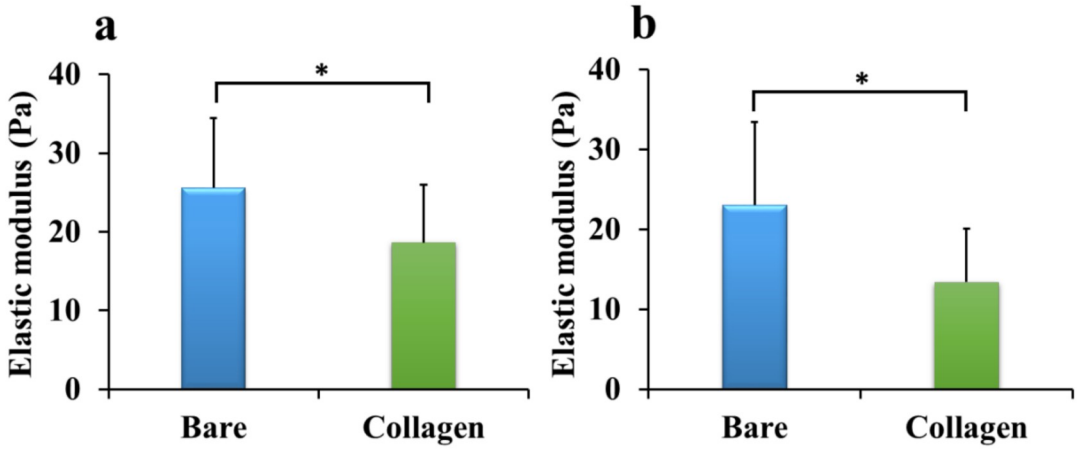

Figure 3.12: Mean values of elastic modulus for (a) indentation and (b) retraction.(Nb, Nc = 26; $p < 0.01$ (t-test)).

Box plot representation of the elastic modulus values tells more about the data distribution as shown in Figure 3.13. Notice that while the 50 % clusters (2 nd+3rd quartiles) are quite similar in dimension for all cases, the elastic modulus data for bare substrates have more spread than those for collagen coated substrates. A t-test has been applied to show the data sets are significantly different ($p< 0.01$).

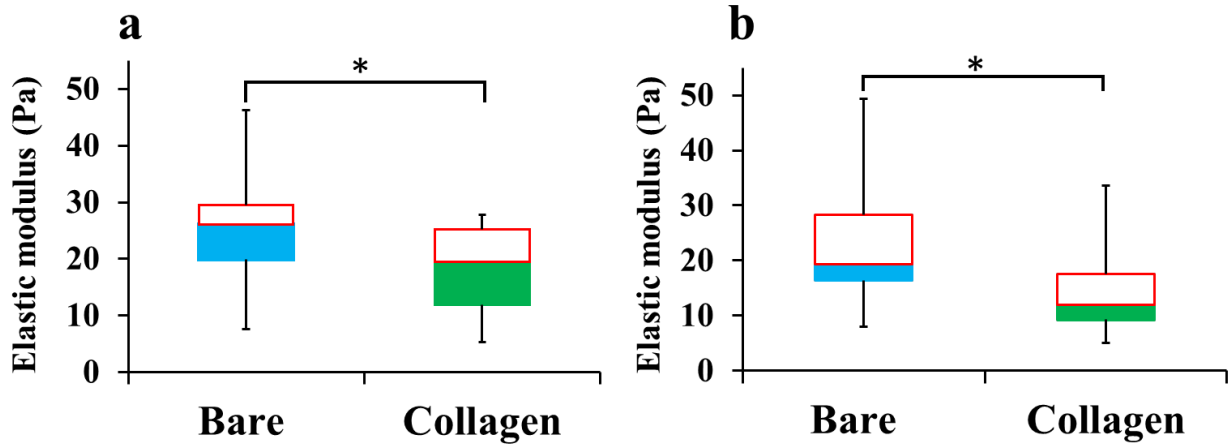

Figure 3.13: Box plot representation of the distribution of elastic modulus values for **(a)** indentation and **(b)** retraction. (Nb, Nc =26; p<0.01(t-test))

3.2.3 Discussion

The cell's morphology on glass and collagen coated substrates showed that cells cultured on glass spread more than those cultured on collagen (see **Figure 3.14**). These morphological changes can be linked with the organization of cell cytoskeleton, showing that cells respond to extra-cellular environmental changes. Cytoskeleton re-arrangement is also accompanied by variations of cell spreading and motility. For instance, cells on compliant substrates exhibit reduced spreading, greater migration rates, and elevated lamellipodial activity compared with cells on more rigid substrates (Pelham and Wang 1997). Increased motility and lamellipodial activity on compliant substrates is associated with more dynamic focal adhesions, whereas cells on rigid substrates had more regularly shaped, stable adhesions (Fischer et al. 2012; Khademhosseini 2008; Engler et al. 2004).

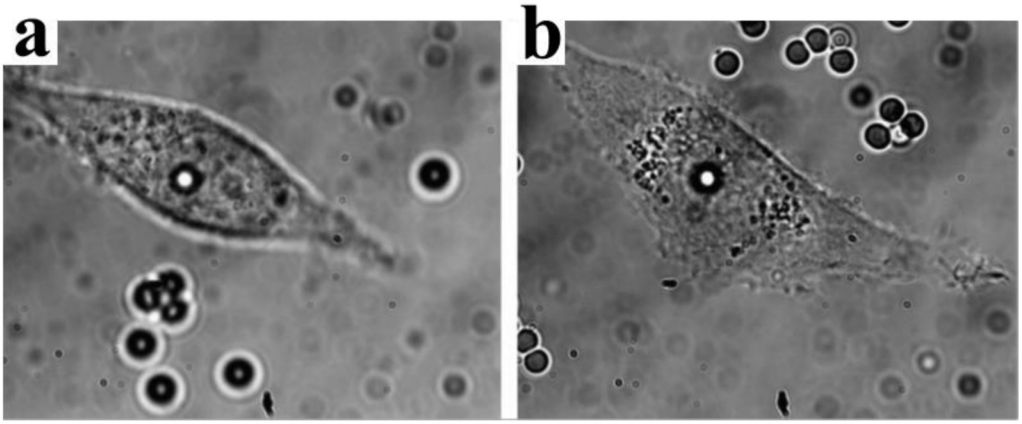

Figure 3. 14 Optical image of morphological changes of HBL-100 cells cultured on **(a)** collagen coated and **(b)** bare substrate.

3.2.4 Conclusion

We studied the effect of substrate stiffness on the elastic behavior of three breast cell lines, HBL-100, MCF-7 and MDA-MB-231. Cells were cultured on PDMS coated glass having stiffnesses as 173kPa, 88kPa and 17kPa. Our results show that cell senses the underlying substrate stiffness and modify its elasticity accordingly. It is shown that HBL-100 and MCF-7 gets softer on complaint substrates while MDA-MB-231 exhibits increase in elasticity. The morphology of these cells on PDMS substrates shows that HBL-100 and MCF-7 adopt a compact structure on soft PDMS substrate while MDA-MB-231 shows polarization and greater lamellopodia activity (about 70 % of the MDA-MB-231cells shows polarization). The correlations of morphology and elasticity

values are directly connected with a cells aggressiveness. Metastatic cells, MDA-MB-231, are stiffer on soft substrate because they have the ability to apply forces on the compliant substrate and apply greater traction forces, which in term increase the cytoskeleton stiffness. While, HBL-100 and MCF-7 cells are passive and adapts to the compliance of the substrate. When HBL-100 cells were plated on collagen coated substrate, they showed decrease in elasticity and adopted a compact morphology. Our result demonstrate that substrate stiffness plays a dominant role in cell function and morphology. In conclusion, cell elasticity changes with substrate stiffness can be used as marker to distinguish between types of cells with different cancer aggressiveness.

3.3 EFFECT OF NEIGHBORING CELLS ON CELL STIFFNESS

A tissue to function normal, all its interconnected cells should work in a well-coordinated way. Cells constantly sense mechanical forces from their neighboring cells that play a pivotal role in cell functions (Schoen et al. 2013; Mierke 2014)Any mechanical abnormality and aberrant signals are either compensated by the neibhouring cells or they may hinder the normal tissue function. Evidences indicate (Kamińska et al. 2015) that mechanical interaction between normal and neoplastic cell contributes to tumor growth.

This section is dedicated to cell-cell interaction dynamics for the three breast cancer cell lines. Cell-cell interaction is another important constituent of the mechanical interaction mechanism with microenvironment (Rodriguez et al. 2013). It has a prime importance for the fundamental understanding of metastasis and cell behavior in malignant conditions. Cell-cell interactions are complex and includes cell–cell interactions in normal tissues, primary tumor, interactions during transit at metastasis stage and secondary tumor site (Bacac and Stamenkovic 2008) (Bershadsky et al. 2003). Initiation, detachment and organ-specific affinity of cancer cells to host cells in terms of mechanical interaction can reveal deeper understanding of cancer progression and metastasis (Subra Suresh, 2007; Makale, 2007) (Brunner et al. 2006; Wolf and Friedl 2006).

3.3.1 Effects of cell-cell connection on cell mechanics

To investigate cell stiffness modulation during interactions with neighboring cells, we analyzed cell lines in contact conditions **(Figure 3.14).** All the three cell lines were cultured on the same type of glass cover slips, which act as hard substrate to the cells (~ GPa of stiffness). Since the cell senses it's surrounding, to understand the effects of neighboring cells on the mechanical properties

of the cell under study, they were cultured with varying densities (see section **Material and Methods**) to get cells in contact. An isolated cell is not touching any other cell while a connected cell has at least two contacts with the neighboring cells. Those surrounding cells act as mechanical cage to the cell.

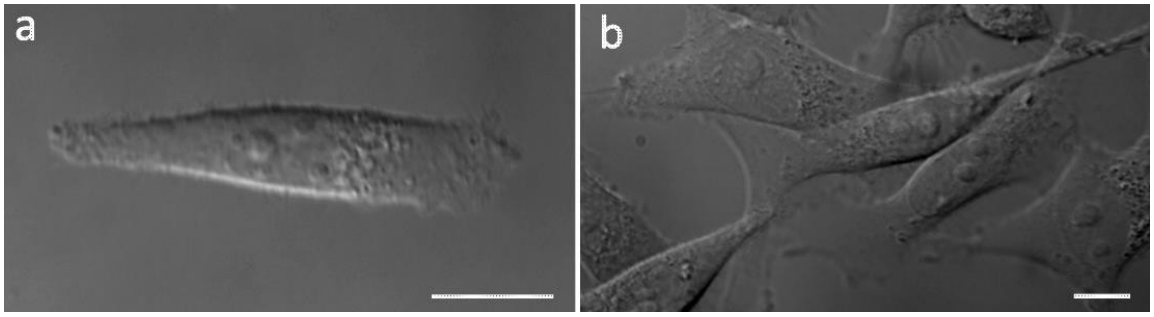

Figure 3.15: MDA-MB-231 cells cultured on glass substrate. Cell is categorized as **(a)** isolated cell: when there is no interaction with any other cell and **(b)** Connected: when the cell interact with two or more cells. Scale bars 10 µm.

Table 3.5: Elastic modulus measurements (± standard deviation) for all three cell lines measured in connected condition in three different cellular sub-regions. (L1, L2 and L3).

	Cell stiffness at cellular sub-regions in connected condition					
	HBL-100		**MCF-7**		**MDA-MB-231**	
	E (Pa) ±SD	**n**	**E (Pa) ±SD**	**n**	**E (Pa) ±SD**	**n**
L1	**30** ± 11	29	20 ± 11	15	31 ± 12	14
L2	**25** ± 9		18 ± 11		27 ± 12	
L3	**21** ± 8		14 ± 7		23 ± 11	

When the three cell lines are indented at the center (nuclear region, L1) in connected conditions the prominent variation in elasticity has been observed. **Figure 3.15** shows the comparative bar plot of the three cell lines. In connected conditions, the most aggressive cell line MDA-MD-231 becomes stiffer while HBL-100 stiffness decreases. MCF-7 on other hand becomes softer in connected conditions. These results show that the neibhouring cells has profound effect on the cells.

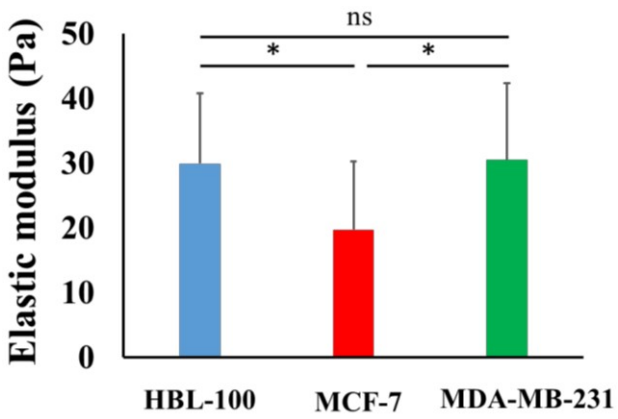

Figure 3.16: Bar plot representation of Elastic modulus values for the three cell lines indented at the nuclear region in connected condition. MDA-MB-231 is no softer in connected condition (as it was in isolated condition), having similar elasticity as HBL-100. MCF-7 has significantly lower (* P: <0.05) elastic modulus than the other two cell lines.

Prominent variation in stiffness was observed as summarized in **Table 3.5** and shown in **Figure 3.17**. Stiffness of HBL-100 and MCF-7 cells decreases by (17%, 10%) and (30%, 30%), while for MDA-MB-231 it decreases by 13% and 26% at cytoplasm and leading edge region as compared with the nuclear region. Results **(Figure 3.17, Table 3.5)** show that even in contact conditions, the leading edge has significantly lower stiffness than the nuclear region.

In connected condition MD-MB-231 is no more a softer one and its stiffness is comparable with HBL-100 in all the three locations. MCF-7 exhibits a softer character. For the three cell lines, cell stiffness in cytoplasm and the leading edges is almost uniform and loses statistical significance. This may be due to the fact that during cell-cell interactions the cytoskeleton organization is more dynamic, leading to a reduction in stiffness variance.

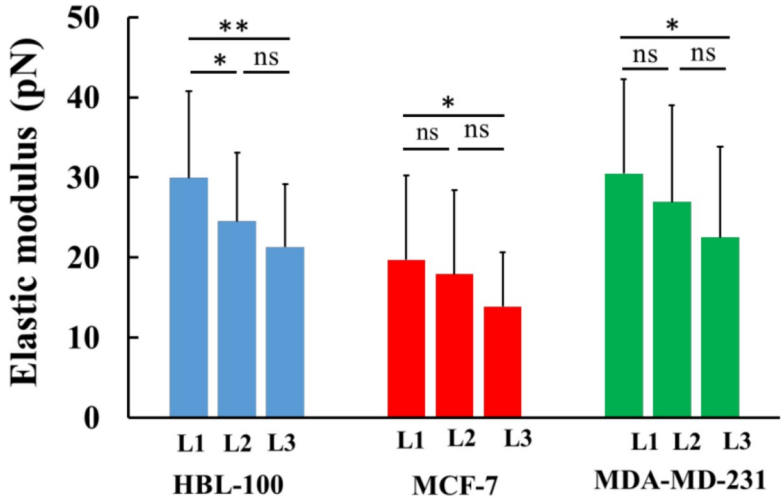

Figure 3.17: Elastic modulus values for the analyzed cell lines indented at three cellular locations in connected conditions. Stiffness decreases from nuclear region to the leading edge. Cell lines exhibit the same stiffness in the cytoplasm and leading edge indicating that cell cytoskeleton organization during interactions becomes more dynamic. MDA-MB-231 shows the same stiffness as HBL-100. (t-test:*$p < 0.05$, **$p < 0.01$).

3.3.2 Comparison of elasticity in isolated and connected conditions

Stiffness values corresponding to regional locations in isolated and connected conditions show a decreasing trend for HBL-100 and MCF-7, whereas MDA-MB-231 becomes stiffer during cell-cell interaction as shown in **Figure 3.18**. For HBL-100 and MCF-7 stiffness at nuclear region decreases by an amount of 17% and 49% respectively. MDA-MB-231 responds opposite, it becomes stiffer in contact condition. Stiffness increases by 39%, 41% and 57% in L1, L2 and L3 locations respectively. The higher increment at the leading edge in interactive condition demonstrates that MD-MB-231 orchestrates more cytoskeletal components (Kristal-Muscal et al. 2013) at the leading edge and applies greater force on the membrane. In contact condition MDA-MB-231becomes stiffer and its stiffness is comparable with HBL-100 **(Table 3.4)** while MCF-7 turns softer (**Figure 3.18**).

HBL-100 and MDA-MB-321cells do not express E-cadherins, which is involved in cell-cell tight junctions, whereas MCF-7 does express them, hence they have different interaction mechanisms (Guo et al. 2014; Lee et al. 2012) · Furthermore, HBL-100 (non-tumorigenic) and MCF-7 (tumorigenic) are noninvasive, but MDA-MB-321 is invasive, therefore their response to the interacting cells might be different. Lee *et al* have shown that MDA-MB-231 cells are more mobile

in active interaction environment of MCF-10A (non-tumorigenic epithelial cell line/normal counterpart of MCF-7) monolayer as compared to non-invasive MCF-7 cells (Lee et al. 2012) They showed that invasive cells (MDA-MB-321) are softer and more sensitive to physical forces if applied on the lateral surfaces of the cells. Our results show that MDA-MB-231 is stiffer in interacting environment whereas the MCF-7 and HBL-100 turns softer during cell-cell interactions, in agreement Kristal *et al,* (Kristal-Muscal et al. 2013) who demonstrated that cell with metastatic potential (MDA-MD-231) generates greater forces despite their soft character as compared to low metastatic potential cell (MDA-MB-468) and benign cells (MCF-10A), which don't indent the substrate at all.

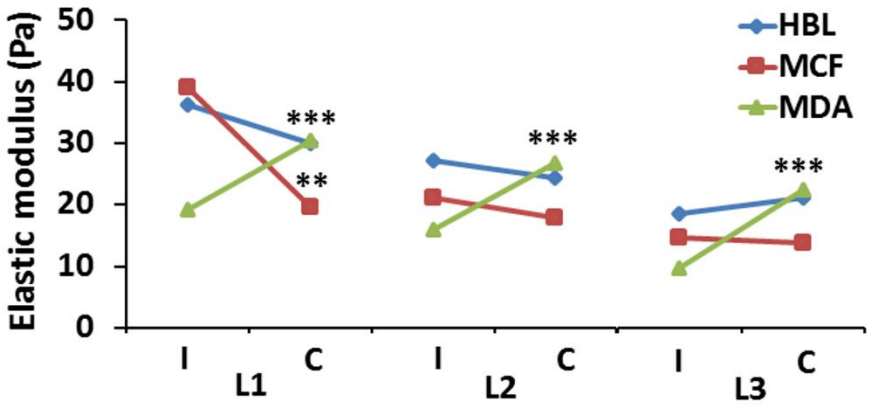

Figure 3.18: Elastic moduli variation in isolated (I) and connected (C) conditions in nuclear (L1), cytoplasm (L2) and leading edge (L3) regions. MDA-MB-231 exhibits a more prominent variation in connected conditions as compared to HBL-100 and MFC-7. (t-test: **p < 0.01, ***p < 0.001).

3.3.3 Discussion

Cancer cell metastasis formation is a complicated mechanism and is the main cause of death in many cancer patients. Evidence indicates that in cancer microenvironment, ECM becomes stiffer as compared to its normal state, but cells behave softer (Katira et al. 2013) and exhibits increased acto-myosin cortex contractility (Kristal-Muscal et al. 2013). Furthermore, some studies show that by altering the mechanics of cell microenvironment, cancerous cell may act as normal ones (Bissell and Hines 2011; Ingber 2008). Herein our approach demonstrates that cell-cell connection modifies cells mechanical behavior. In the same micro environmental conditions HBL-100 and MCF-7 cells were getting softer by interacting with their neighboring cells, but MDA-MB-231

cells became stiffer. In isolated conditions, cell adopts a particular structure and morphology on a harder substrate (glass), and the same stiffness feature has been shown for all the analyzed cell lines. When they feel dynamic interactions (cell-cell cross talk) they rearrange their cytoskeleton and those changes are intrinsic for each cell line depending on the level of its aggressiveness.

Surrounding cells act like a steric cage that restricts the mechanical movement of the cell (Lee et al. 2012). Stiffness increase in MDA-MB-231 during interaction may be attributed to the strong forces its cytoskeleton applies on the leading edge of the membrane (as increase by a factor of 2.3x) to push against the steric mechanical barrier (**Figure 3.17**). As compared to MCF-7 cells, which are tumorigenic but not metastatic, they behave as isolated. MCF-7 cell cytoskeleton tends to be more uniformly distributed in terms of stiffness during cell–cell interaction. This difference may arise as MDA-MB-231 cells are more sensitive to the physical forces because of increased actomyosin contractility, and because they lack permanent adherent junctions.MCF-7 cells form E-cadherins based adherent junctions and thus activated myosin II generates tugging forces to prevent impinging forces (Lee et al. 2012). Cadherin based junctions prevent MCF-7 cells to experience full contact force as in case of MDA-MB-231 cell-cell interactions. Interactions with neighboring cells make HBL-100 cells softer but a bit stressed at the leading edge. As, HBL-100 and MDA-MB-231 do not form permanent junctions, their migratory behavior is influenced by the surrounding cells, which apply forces on the neighboring cells and we detect these forces as change in stiffness. This phenomenon, leads HBL-100 to soften and MDA-MB-231 to stiffen. These dynamic variations in stiffness of invasive cells in interactive condition highlight the fact that cell alter internal cytoskeletal organization to proliferate and metastasize, they can apply forces to push the barrier but at the same time they can change the morphology to penetrate.

Our results show that measurements region on the cell influences results: stiffness decreases from the center towards the periphery (leading edge). Single cell mechanical measurements greatly change with cellular sub-regions and should be considered while measuring and comparing cells elasticities.

3.3.4 Conclusion

OT is a powerful force spectroscopic technique, capable of applying and measuring pN forces. This capability was utilized to study stiffness variations in cell in interacting conditions. We studied the three cell lines in connected conditions with other neibhouring cells the same type.

MDA-MD-231 is considered to be softer in isolated conditions but when it interact with other cells it shows increase in stiffness comparable to HBL-100.This increase in stiffness maybe attributed to high acto-myosin contractile capability of metastatic cells and increased motility. HBL-100 and MCF-7 on other hand have shown decease in stiffness. In connected conditions all the three cell lines loss regional variation in stiffness, indicating that cells interior cytoskeleton is actively involved during interaction with other cells. More rigorous mechanical studies on cancer cells corresponding to different range of forces and different micro-environmental conditions may further unravel aspects of cancer progression and metastasis formation. In future studies, we will apply this technique to investigate effects of ECM on cell-cell interaction and to study the related mechanotransduction pathways.

Conclusions and Final Remarks

The intrinsic ability of cells to sense and respond to any mechanical changes in its microenvironment give us the opportunity to develop new biophysical tools to manipulate the cells state in different microenvironmental conditions. Mechanical properties of cell are being used as prominent biomarkers for cell phenotyping in cancer and disease diagnosis. Viscoelasticity is among the most studied mechanical properties of cells. Cancer cells exhibit alterations in viscoelastic properties at different level of cancer progression. There are several biophysical techniques available in the scientific community to study viscoelastic properties of cells, everyone has its own application regime and benefits in terms of force range and time scale.

The main goal of this thesis was to develop an optical tweezers (OT) force spectroscopy technique to validate the cell elasticity parameter as a label free marker of cancer cells in different microenvironmental conditions.

For this purpose we considered three breast cell lines in different progression states of cancer and tried to distinguish them on the basis of their elasticity. We studied the alterations in cell elasticity in different microenvironmental conditions by changing the substrate stiffness and cell neibhouring.

We used three cell lines as model:

- HBL-100, as a control, derived from a woman with no breast cancer lesion;
- MCF-7, a tumor cell representing the luminal A breast cancer subtype;
- MDA-MB-231, a highly aggressive cell lines representing the basal cancer subtype.

We introduced the OT vertical indentation approach to study cell elasticity using Hertz model in a similar way as for AFM cell indentation experiment. We applied two mechanisms to calculate cell elasticity from force-indentation curves: fixed indentation and fixed force range. In fixed indentation we fix the indentation (e.g. 200 nm) in a linear range of Force-indentation curve, while in fixed force method we set the range of force from min (e.g. $0.15F_{max}$) to max (e.g. $0.75F_{max}$) similar to AFM data analysis. Furthermore, we used 3D particle tracking with QPD and back focal plane interferometry to calculate also the lateral forces which arise during the vertical indentation of the cell. These lateral forces are usually ignored by other reported indentation techniques because of the technique's limitation itself (AFM) or because the detector limitation (a single

photodiode instead of QPD). We studied the vertical and lateral forces contribution and found that indeed the lateral forces are not negligible and should be considered for an accurate analysis of the cell elasticity. The contributions of lateral forces in understanding different aspects of mechanical properties of cell membrane will be exploited in future studies.

Applying OT vertical indentation and considering the vertical force component we calculated the cell elasticity and compared cells from the three cell lines above mentioned.. We found that metastatic cells (MDA-MD-231) are softer than HBL-100 and MCF-7 cells when measured cells are isolated and cultured on bare glass. Our probing force is in the range of 10 pN and the obtained elasticity in the Pa range. We performed AFM indentation with nN force for the same types of cells and found that the elastic moduli values were in the kPa range. Both techniques indicate the same trend for the three cell lines, showing that OT reveals the elastic behavior and can be used as complementary technique to AFM in low force regime. We extended our approach to study different regions of the cell and we showed that all the three cell lines exhibit descending trend in elasticity from the cell nucleus towards the leading edge. The nuclear (center) region appeared as the stiffer part of the cell and provides the most meaningful results for cell indentation studies. We compared our results with AFM and found that both techniques show the same trends in cell regional mechanical variations.

Normal tissue cells are anchorage dependent, and once grown on a substrate with defined stiffness, cells adapt their own elasticity to the stiffness of their extra cellular matrix (ECM). We studied the effects of substrate compliance on the cell elasticity. In lab-based experiments, cell are seeded on glass substrate having higher elastic modulus ($E \approx$ GPa). Therefore, to change the stiffness of the underlying substrate we coated the glass coverslips with three different PDMS having stiffnesses as 173 kPa, 88 k Pa, and 17 kPa. Our results show that all the three cell lines have good adhesion on the three types of PDMS substrates. HBL-100 and MCF-7 show compact morphology while MDA-MB-231 shows polarization and higher lamellopodia motility. HBl-100 and MCF-7 elasticity decreases with the decrease in stiffness of the substrate while MBA-MB-231 becomes stiffer with the decrease in PDMS stiffness. This increase in elasticity may be attributed to the high metastatic potential and cell's ability to apply normal forces on soft substrates. Metastic cells are more motile and exhibit more acto-myosin contractility. We also used Collagen as soft substrate to study the elasticity of HBL-100 cells. HBL-100 adopts a compact morphology on collagen coated glass and show reduced elasticity as compared to glass substrate. These results demonstrate

that cells are responsive to the rigidity of the substrate on which they are cultured and can be used as a marker to distinguish and characterize metastatic cells. In future studies, anchorage dependent focal adhesions and their mechanotransduction pathways and consequent cytoskeletal alterations will be analyzed.

The tissue cells not only feel the mechanical changes in their ECM but they are also connected with their neibhouring cells, and transmit mechanical signals to their neibhouring cells in a coordinated way. To investigate the cell stiffness modulation during interactions with neighboring cells, we analyzed cell lines in contact conditions. In isolated conditions, MDA-MB-231 is softer as compared HBL-100 and MCF-7 but the situation changes when MDA-MB-231 cells interact with other cells. In this case the stiffness increases and becomes comparable to HBL-100 in connected conditions, meaning that an MDA-MB-231 metastatic cell surrounded by other cells gets more aggressive as these surrounding cells provide a mechanical blockage to its motility. This increase in stiffness maybe attributed to high acto-myosin contractile capability of metastatic cells and increased motility (Guo et al. 2014; Lee et al. 2012; Kristal-Muscal et al. 2013; Kraning-Rush et al. 2012). HBL-100 and MCF-7 on other hand have shown decrease in stiffness. Also, the regional variation in mechanical properties were studied in connected conditions and results show that all the three cell lines loss regional variation in stiffness, indicating that cells interior cytoskeleton is actively involved during interaction with other cells. Following the same protocol, we will investigate the behavior of these cells in mixed coculture and the related signaling pathways.

In summary, using OT we are able to apply well-calibrated pN forces and study small changes in the elasticity of cells. Vertical indentation measurements of the three cell lines in isolated and connected conditions as well as on bare glass and PDMS show promising results. MDB-MB-231 cells are metastatic and when they feel soft underlying substrate or the neibhouring cells their response is more aggressive, i.e increasing in elasticity, which is linked to the interior cytoskeleton of the cells. HBL-100 and MDA-BM-231 cells get softer on compliant cells and also when surrounded by other cells of the same type. More rigorous mechanical studies on cancer cells corresponding to different range of forces and different micro-environmental conditions may further unravel aspects of cancer progression and metastasis formation.

Acknowledgements

My graduate life at UNITS was enjoyable. My past three years in Trieste were the most challenging and adventurous. These lifelong experiences both academic and cultural, undoubtedly, will shine my potentials. I want to say thanks to many nice people for their encouragement, support and help throughout this journey.

I would like to express deepest gratitude to my supervisor Dr. Dan Cojoc, who gave me the opportunity to work in his group and offered me freedom during my research. I was extremely lucky to have Dr. Dan Cojoc as thesis supervisor, his considerate encouragement has been a great source of my 'careless' bravery in handling Optical Tweezers experiments.

I would like to thank all the other members of the OM-Lab, especially Giovanna Coceano, Leonardo Venturelli, Alberto Mariutti, Ladan Amin and Fedrico Iseppon; every time I needed them, they were willing to help me.

My deepest regards for Professor Giacinto Scoles, who supported my project. He inspired me always whenever I got the opportunity to meet him.

A big thanks to all the colleagues of the "LILIT" group, but in particular to Alessandra, Nicola and Farideh, there smiling and joyful attitudes are always refreshing and relieving.

Heartiest thanks to Dr. Roberta Ferranti for solving many bureaucratic and domestic issues.

I would like to thank two people who supported me alot: Dr. Sajid Hussain, who welcomed me and is the reason why I am here in Trieste now; Rafaqat Hussain, for his generous help and kind attitude and tasty recipes. We spent really great time in the same apartment just like brothers. Thanks to Raheemullah and Majid Ali for being so much supportive and helping. I thank all the members of the Trieste Cricket Club for providing me opportunities to play cricket.

Thanks to Indian and Pakistani friends especially Zain & Shama, Hashim & Asma, Sunil & Merlyn, Naila & Ikram, for their welcoming attitudes and organizing multiple gatherings.

Thanks to Shahid Nawaz for sharing the best days and the jogging hours we spent together at Barcola. Special thanks to Dr. Bushra for her kind moral support and advices in research.

I would like to thanks Rabail for her criticism during my thesis writing, her criticism give me the courage to write well and fast.

I am also grateful to many people in Pakistan for their prayers and best wishes. I want to thanks Dr. M. Ateeq for sharing scientific and social views. Special Thanks are to Dr. Shahid Ali, a true and sincere friend, he is always besides me whenever I need him. I want to thank my dearest Uncle, Ali Bahadar, for constant encouragement and inspiration.

Finally, I thank my sisters and brother for their unconditional support and love. I miss your company and your smiles. I want to say thanks to my two ideals, my father, his untiring personality always give me the strength to work hard and, my mother, without her endless blessings and prayers I would not be able to become who I am.

Muhammad Sulaiman Yousafzai
Trieste, 26-02-2016

References

Allemand, J.-F., D. Bensimon, and V. Croquette. 2003. Stretching DNA and RNA to probe their interactions with proteins. *Current opinion in structural biology* 13 (3):266-274.

Ashkin, A. 1970. Acceleration and trapping of particles by radiation pressure. *Physical review letters* 24 (4):156.

Ashkin, A., and J. Dziedzic. 1987. Optical trapping and manipulation of viruses and bacteria. *Science* 235 (4795):1517-1520.

Ashkin, A., J. Dziedzic, J. Bjorkholm, and S. Chu. 1986. Observation of a single-beam gradient force optical trap for dielectric particles. *Optics letters* 11 (5):288-290.

Ashok, P. C., and K. Dholakia. 2012. Optical trapping for analytical biotechnology. *Current opinion in biotechnology* 23 (1):16-21.

Bacac, M., and I. Stamenkovic. 2008. Metastatic cancer cell. *Annu. Rev. pathmechdis. Mech. Dis.* 3:221-247.

Bao, G., and S. Suresh. 2003. Cell and molecular mechanics of biological materials. *Nature materials* 2 (11):715-725.

Bausch, A., and K. Kroy. 2006. A bottom-up approach to cell mechanics. *Nature physics* 2 (4):231-238.

Bershadsky, A. D., N. Q. Balaban, and B. Geiger. 2003. Adhesion-dependent cell mechanosensitivity. *Annual review of cell and developmental biology* 19 (1):677-695.

Bissell, M. J., and W. C. Hines. 2011. Why don't we get more cancer? A proposed role of the microenvironment in restraining cancer progression. *Nature medicine* 17 (3):320-329.

Block, S. M., L. S. Goldstein, and B. J. Schnapp. 1990. Bead movement by single kinesin molecules studied with optical tweezers.

Bodensiek, K., W. Li, P. Sánchez, S. Nawaz, and I. A. Schaap. 2013. A high-speed vertical optical trap for the mechanical testing of living cells at piconewton forces. *Review of Scientific Instruments* 84 (11):113707.

BRUKER. *http://www.bruker.com/products/surface-analysis/atomic-force-microscopy.html*.

Brunner, C. A., A. Ehrlicher, B. Kohlstrunk, D. Knebel, J. A. Käs, and M. Goegler. 2006. Cell migration through small gaps. *European Biophysics Journal* 35 (8):713-719.

Bustamante, C., Z. Bryant, and S. B. Smith. 2003. Ten years of tension: single-molecule DNA mechanics. *Nature* 421 (6921):423-427.

Cai, D., A. Neyer, R. Kuckuk, and H. Heise. 2008. Optical absorption in transparent PDMS materials applied for multimode waveguides fabrication. *Optical materials* 30 (7):1157-1161.

Carter, S. B. 1967. Haptotaxis and the mechanism of cell motility. *Nature* 213:256-260.

Cattaruzza, M., C. Lattrich, and M. Hecker. 2004. Focal adhesion protein zyxin is a mechanosensitive modulator of gene expression in vascular smooth muscle cells. *Hypertension* 43 (4):726-730.

Chan, C. E., and D. J. Odde. 2008. Traction dynamics of filopodia on compliant substrates. *Science* 322 (5908):1687-1691.

Chen, W.-H., S.-J. Cheng, J. T. Tzen, C.-M. Cheng, and Y.-W. Lin. 2013. Probing relevant molecules in modulating the neurite outgrowth of hippocampal neurons on substrates of different stiffness. *PLoS one* 8 (12):e83394.

Cheng, G., J. Tse, R. K. Jain, and L. L. Munn. 2009. Micro-environmental mechanical stress controls tumor spheroid size and morphology by suppressing proliferation and inducing apoptosis in cancer cells. *PLoS one* 4 (2):e4632.

Chien, S. 2007. Mechanotransduction and endothelial cell homeostasis: the wisdom of the cell. *American Journal of Physiology-Heart and Circulatory Physiology* 292 (3):H1209-H1224.

Chiou, Y.-W., H.-K. Lin, M.-J. Tang, H.-H. Lin, and M.-L. Yeh. 2013. The influence of physical and physiological cues on atomic force microscopy-based cell stiffness assessment. *PLoS one* 8 (10).

Coceano, G., M. Yousafzai, W. Ma, F. Ndoye, L. Venturelli, I. Hussain, S. Bonin, J. Niemela, G. Scoles, and D. Cojoc. 2016. Investigation into local cell mechanics by atomic force microscopy mapping and optical tweezer vertical indentation. *Nanotechnology* 27 (6):065102.

Costa, K. D. 2004. Single-cell elastography: probing for disease with the atomic force microscope. *Disease markers* 19 (2-3):139-154.

Cross, S. E., Y.-S. Jin, J. Rao, and J. K. Gimzewski. 2007. Nanomechanical analysis of cells from cancer patients. *Nature nanotechnology* 2 (12):780-783.

Cross, S. E., Y.-S. Jin, J. Tondre, R. Wong, J. Rao, and J. K. Gimzewski. 2008. AFM-based analysis of human metastatic cancer cells. *Nanotechnology* 19 (38):384003.

Dalby, M. J., M. O. Riehle, D. S. Sutherland, H. Agheli, and A. Curtis. 2005. Morphological and microarray analysis of human fibroblasts cultured on nanocolumns produced by colloidal lithography. *Eur Cell Mater* 9 (1).

Dao, M., C. Lim, and S. Suresh. 2003. Mechanics of the human red blood cell deformed by optical tweezers. *Journal of the Mechanics and Physics of Solids* 51 (11):2259-2280.

Discher, D. E., P. Janmey, and Y.-l. Wang. 2005. Tissue cells feel and respond to the stiffness of their substrate. *Science* 310 (5751):1139-1143.

DuFort, C. C., M. J. Paszek, and V. M. Weaver. 2011. Balancing forces: architectural control of mechanotransduction. *Nature reviews Molecular cell biology* 12 (5):308-319.

Dy, M.-C., S. Kanaya, and T. Sugiura. 2013. Localized cell stiffness measurement using axial movement of an optically trapped microparticle. *Journal of biomedical optics* 18 (11):111411-111411.

Engler, A., L. Bacakova, C. Newman, A. Hategan, M. Griffin, and D. Discher. 2004. Substrate compliance versus ligand density in cell on gel responses. *Biophysical journal* 86 (1):617-628.

Engler, A. J., S. Sen, H. L. Sweeney, and D. E. Discher. 2006. Matrix elasticity directs stem cell lineage specification. *Cell* 126 (4):677-689.

Fischer, R. S., K. A. Myers, M. L. Gardel, and C. M. Waterman. 2012. Stiffness-controlled three-dimensional extracellular matrices for high-resolution imaging of cell behavior. *Nature protocols* 7 (11):2056-2066.

Friedl, P., and D. Gilmour. 2009. Collective cell migration in morphogenesis, regeneration and cancer. *Nature reviews Molecular cell biology* 10 (7):445-457.

Friedl, P., Y. Hegerfeldt, and M. Tusch. 2004. Collective cell migration in morphogenesis and cancer. *International Journal of Developmental Biology* 48:441-450.

Fu, J., Y.-K. Wang, M. T. Yang, R. A. Desai, X. Yu, Z. Liu, and C. S. Chen. 2010. Mechanical regulation of cell function with geometrically modulated elastomeric substrates. *Nature methods* 7 (9):733-736.

Gardel, M., F. Nakamura, J. Hartwig, J. C. Crocker, T. Stossel, and D. Weitz. 2006. Stress-dependent elasticity of composite actin networks as a model for cell behavior. *Physical review letters* 96 (8):088102.

Geiger, T. R., and D. S. Peeper. 2009. Metastasis mechanisms. *Biochimica et Biophysica Acta (BBA)-Reviews on Cancer* 1796 (2):293-308.

Georges, P. C., and P. A. Janmey. 2005. Cell type-specific response to growth on soft materials. *Journal of applied physiology* 98 (4):1547-1553.

Giannone, G., B. J. Dubin-Thaler, H.-G. Döbereiner, N. Kieffer, A. R. Bresnick, and M. P. Sheetz. 2004. Periodic lamellipodial contractions correlate with rearward actin waves. *Cell* 116 (3):431-443.

Gieni, R. S., and M. J. Hendzel. 2008. Mechanotransduction from the ECM to the genome: are the pieces now in place? *Journal of cellular biochemistry* 104 (6):1964-1987.

Gomez, G. A., R. W. McLachlan, and A. S. Yap. 2011. Productive tension: force-sensing and homeostasis of cell–cell junctions. *Trends in cell biology* 21 (9):499-505.

Gou, X., H. C. Han, S. Hu, A. Y. Leung, and D. Sun. 2013. Applying combined optical tweezers and fluorescence microscopy technologies to manipulate cell adhesions for cell-to-cell interaction study. *Biomedical Engineering, IEEE Transactions on* 60 (8):2308-2315.

Grier, D. G. 2003. A revolution in optical manipulation. *Nature* 424 (6950):810-816.

Guck, J., S. Schinkinger, B. Lincoln, F. Wottawah, S. Ebert, M. Romeyke, D. Lenz, H. M. Erickson, R. Ananthakrishnan, and D. Mitchell. 2005. Optical deformability as an inherent cell marker for testing malignant transformation and metastatic competence. *Biophysical journal* 88 (5):3689-3698.

Guilak, F., J. R. Tedrow, and R. Burgkart. 2000. Viscoelastic properties of the cell nucleus. *Biochemical and biophysical research communications* 269 (3):781-786.

Guo, X., K. Bonin, K. Scarpinato, and M. Guthold. 2014. The effect of neighboring cells on the stiffness of cancerous and non-cancerous human mammary epithelial cells. *New Journal of Physics* 16 (10):105002.

Guz, N., M. Dokukin, V. Kalaparthi, and I. Sokolov. 2014. If cell mechanics can be described by elastic modulus: study of different models and probes used in indentation experiments. *Biophysical journal* 107 (3):564-575.

Hall, A. 2005. Rho GTPases and the control of cell behaviour. *Biochemical Society Transactions* 33 (5):891-896.

Hanahan, D., and R. A. Weinberg. 2011. Hallmarks of cancer: the next generation. *Cell* 144 (5):646-674.

Hoffman, B. D., and J. C. Crocker. 2009. Cell mechanics: dissecting the physical responses of cells to force. *Annual review of biomedical engineering* 11:259-288.

Holle, A. W., J. L. Young, and J. P. Spatz. 2015. In vitro cancer cell–ECM interactions inform in vivo cancer treatment. *Advanced drug delivery reviews*.

Hormeño, S., and J. R. Arias -Gonzalez. 2006. Exploring mechanochemical processes in the cell with optical tweezers. *Biology of the Cell* 98 (12):679-695.

Hu, S., J. Chen, and N. Wang. 2004. Cell spreading controls balance of prestress by microtubules and extracellular matrix. *Frontiers in bioscience: a journal and virtual library* 9:2177-2182.

Hu, S., X. Gou, H. Han, A. Y. Leung, and D. Sun. 2013. Manipulating cell adhesions with optical tweezers for study of cell-to-cell interactions. *Journal of biomedical nanotechnology* 9 (2):281-285.

Huang, S., and D. E. Ingber. 2005. Cell tension, matrix mechanics, and cancer development. *Cancer cell* 8 (3):175-176.

Ingber, D. E. 2003. Tensegrity I. Cell structure and hierarchical systems biology. *Journal of cell science* 116 (7):1157-1173.

Ingber, D. E. 2006. Cellular mechanotransduction: putting all the pieces together again. *The FASEB journal* 20 (7):811-827.

Ingber, D. E. 2008. Can cancer be reversed by engineering the tumor microenvironment? Paper read at Seminars in cancer biology.

Ivers, L. P., B. Cummings, F. Owolabi, K. Welzel, R. Klinger, S. Saitoh, O. Darran, Y. Fujita, D. Scholz, and N. Itasaki. 2014. Dynamic and influential interaction of cancer cells with normal epithelial cells in 3D culture. *Cancer cell international* 14 (1):108.

Jaalouk, D. E., and J. Lammerding. 2009. Mechanotransduction gone awry. *Nature reviews Molecular cell biology* 10 (1):63-73.

Jacobs, C. R., H. Huang, and R. Y. Kwon. 2012. *Introduction to cell mechanics and mechanobiology*: Garland Science.

Jaffe, A. B., and A. Hall. 2005. Rho GTPases: biochemistry and biology. *Annu. Rev. Cell Dev. Biol.* 21:247-269.

Janmey, P. A., and D. A. Weitz. 2004. Dealing with mechanics: mechanisms of force transduction in cells. *Trends in biochemical sciences* 29 (7):364-370.

Jemal, A., F. Bray, M. M. Center, J. Ferlay, E. Ward, and D. Forman. 2011. Global cancer statistics. *CA: a cancer journal for clinicians* 61 (2):69-90.

JPK. *http://www.jpk.com/atomic-force-microscopy.27.en.html* [cited. Available from http://www.jpk.com/atomic-force-microscopy.27.en.html.

Kamińska, K., C. Szczylik, Z. F. Bielecka, E. Bartnik, C. Porta, F. Lian, and A. M. Czarnecka. 2015. The role of the cell–cell interactions in cancer progression. *Journal of cellular and molecular medicine* 19 (2):283-296.

Katira, P., R. T. Bonnecaze, and M. H. Zaman. 2013. Modeling the mechanics of cancer: effect of changes in cellular and extra-cellular mechanical properties. *Frontiers in oncology* 3.

Kellermayer, M. S., S. B. Smith, H. L. Granzier, and C. Bustamante. 1997. Folding-unfolding transitions in single titin molecules characterized with laser tweezers. *Science* 276 (5315):1112-1116.

Ketene, A. N., P. C. Roberts, A. A. Shea, E. M. Schmelz, and M. Agah. 2012. Actin filaments play a primary role for structural integrity and viscoelastic response in cells. *Integrative Biology* 4 (5):540-549.

Khademhosseini, A. 2008. *Micro and nanoengineering of the cell microenvironment: technologies and applications*: Artech House.

Kirmizis, D., and S. Logothetidis. 2010. Atomic force microscopy probing in the measurement of cell mechanics. *International journal of nanomedicine* 5:137.

Kobayashi, T., and M. Sokabe. 2010. Sensing substrate rigidity by mechanosensitive ion channels with stress fibers and focal adhesions. *Current opinion in cell biology* 22 (5):669-676.

Kraning-Rush, C. M., J. P. Califano, and C. A. Reinhart-King. 2012. Cellular traction stresses increase with increasing metastatic potential. *PLoS one* 7 (2):e32572.

Kristal-Muscal, R., L. Dvir, and D. Weihs. 2013. Metastatic cancer cells tenaciously indent impenetrable, soft substrates. *New Journal of Physics* 15 (3):035022.

Kumar, S., I. Z. Maxwell, A. Heisterkamp, T. R. Polte, T. P. Lele, M. Salanga, E. Mazur, and D. E. Ingber. 2006. Viscoelastic retraction of single living stress fibers and its impact on cell

shape, cytoskeletal organization, and extracellular matrix mechanics. *Biophysical journal* 90 (10):3762-3773.

Ladoux, B., and A. Nicolas. 2012. Physically based principles of cell adhesion mechanosensitivity in tissues. *Reports on Progress in Physics* 75 (11):116601.

Laura Andolfi, E. B., Elisa Migliorini, Anita Palma, Anja Pucer, Miran Skrap, Giacinto Scoles, Antonio P. Beltrami, Daniela Cesselli, Marco Lazzarino. 2014. Investigation of Adhesion and Mechanical Properties of Human Glioma Cells by Single Cell Force Spectroscopy and Atomic Force Microscopy. *PloS one (accepted)*.

Lee, M.-H., P.-H. Wu, J. R. Staunton, R. Ros, G. D. Longmore, and D. Wirtz. 2012. Mismatch in mechanical and adhesive properties induces pulsating cancer cell migration in epithelial monolayer. *Biophysical journal* 102 (12):2731-2741.

Lekka, M., K. Pogoda, J. Gostek, O. Klymenko, S. Prauzner-Bechcicki, J. Wiltowska-Zuber, J. Jaczewska, J. Lekki, and Z. Stachura. 2012. Cancer cell recognition–mechanical phenotype. *Micron* 43 (12):1259-1266.

Li, Q., G. Lee, C. Ong, and C. Lim. 2008. AFM indentation study of breast cancer cells. *Biochemical and biophysical research communications* 374 (4):609-613.

Lim, C., E. Zhou, A. Li, S. Vedula, and H. Fu. 2006. Experimental techniques for single cell and single molecule biomechanics. *Materials Science and Engineering: C* 26 (8):1278-1288.

Lim, C. T., A. Bershadsky, and M. P. Sheetz. 2010. Mechanobiology. *Journal of The Royal Society Interface*:rsif20100150.

Liu, B., T.-J. Kim, and Y. Wang. 2010. Live cell imaging of mechanotransduction. *Journal of The Royal Society Interface* 7 (Suppl 3):S365-S375.

Lo, C.-M., H.-B. Wang, M. Dembo, and Y.-l. Wang. 2000. Cell movement is guided by the rigidity of the substrate. *Biophysical journal* 79 (1):144-152.

Maniotis, A. J., C. S. Chen, and D. E. Ingber. 1997. Demonstration of mechanical connections between integrins, cytoskeletal filaments, and nucleoplasm that stabilize nuclear structure. *Proceedings of the National Academy of Sciences* 94 (3):849-854.

Medalsy, I. D., and D. J. Mu ̈ller. 2013. Nanomechanical properties of proteins and membranes depend on loading rate and electrostatic interactions. *ACS nano* 7 (3):2642-2650.

Mierke, C. T. 2014. The fundamental role of mechanical properties in the progression of cancer disease and inflammation. *Reports on Progress in Physics* 77 (7):076602.

Moffitt, J. R., Y. R. Chemla, S. B. Smith, and C. Bustamante. 2008. Recent advances in optical tweezers. *Biochemistry* 77 (1):205.

Murrell, M., R. Kamm, and P. Matsudaira. 2011. Substrate viscosity enhances correlation in epithelial sheet movement. *Biophysical journal* 101 (2):297-306.

Narumiya, S., M. Tanji, and T. Ishizaki. 2009. Rho signaling, ROCK and mDia1, in transformation, metastasis and invasion. *Cancer and Metastasis Reviews* 28 (1-2):65-76.

Nawaz, S., P. Sánchez, K. Bodensiek, S. Li, M. Simons, and I. A. Schaap. 2012. Cell visco-elasticity measured with AFM and optical trapping at sub-micrometer deformations. *PLoS one* 7 (9):e45297.

Neuman, K. C., and S. M. Block. 2004. Optical trapping. *Review of Scientific Instruments* 75 (9):2787-2809.

Neuman, K. C., and A. Nagy. 2008. Single-molecule force spectroscopy: optical tweezers, magnetic tweezers and atomic force microscopy. *Nature methods* 5 (6):491-505.

Odde, D. J., L. Ma, A. H. Briggs, A. DeMarco, and M. W. Kirschner. 1999. Microtubule bending and breaking in living fibroblast cells. *Journal of cell science* 112 (19):3283-3288.

Orr, A. W., B. P. Helmke, B. R. Blackman, and M. A. Schwartz. 2006. Mechanisms of mechanotransduction. *Developmental cell* 10 (1):11-20.

Paszek, M. J., N. Zahir, K. R. Johnson, J. N. Lakins, G. I. Rozenberg, A. Gefen, C. A. Reinhart-King, S. S. Margulies, M. Dembo, and D. Boettiger. 2005. Tensional homeostasis and the malignant phenotype. *Cancer cell* 8 (3):241-254.

Pelham, R. J., and Y.-l. Wang. 1997. Cell locomotion and focal adhesions are regulated by substrate flexibility. *Proceedings of the National Academy of Sciences* 94 (25):13661-13665.

Plant, A. L., K. Bhadriraju, T. A. Spurlin, and J. T. Elliott. 2009. Cell response to matrix mechanics: focus on collagen. *Biochimica et Biophysica Acta (BBA)-Molecular Cell Research* 1793 (5):893-902.

Plodinec, M., M. Loparic, C. A. Monnier, E. C. Obermann, R. Zanetti-Dallenbach, P. Oertle, J. T. Hyotyla, U. Aebi, M. Bentires-Alj, and R. Y. Lim. 2012. The nanomechanical signature of breast cancer. *Nature nanotechnology* 7 (11):757-765.

Pollard, T. D., and J. A. Cooper. 2009. Actin, a central player in cell shape and movement. *Science* 326 (5957):1208-1212.

Raeber, G., M. Lutolf, and J. Hubbell. 2008. Part II: Fibroblasts preferentially migrate in the direction of principal strain. *Biomechanics and modeling in mechanobiology* 7 (3):215-225.

Remmerbach, T. W., F. Wottawah, J. Dietrich, B. Lincoln, C. Wittekind, and J. Guck. 2009. Oral cancer diagnosis by mechanical phenotyping. *Cancer research* 69 (5):1728-1732.

Ridley, A. J. 2006. Rho GTPases and actin dynamics in membrane protrusions and vesicle trafficking. *Trends in cell biology* 16 (10):522-529.

Rodriguez, M. L., P. J. McGarry, and N. J. Sniadecki. 2013. Review on cell mechanics: experimental and modeling approaches. *Applied Mechanics Reviews* 65 (6):060801.

Rother, J., H. Nöding, I. Mey, and A. Janshoff. 2014. Atomic force microscopy-based microrheology reveals significant differences in the viscoelastic response between malign and benign cell lines. *Open biology* 4 (5):140046.

Sahai, E., and C. J. Marshall. 2002. RHO–GTPases and cancer. *Nature Reviews Cancer* 2 (2):133-142.

Schoen, I., B. L. Pruitt, and V. Vogel. 2013. The Yin-Yang of rigidity sensing: how forces and mechanical properties regulate the cellular response to materials. *Annual Review of Materials Research* 43:589-618.

Solon, J., I. Levental, K. Sengupta, P. C. Georges, and P. A. Janmey. 2007. Fibroblast adaptation and stiffness matching to soft elastic substrates. *Biophysical journal* 93 (12):4453-4461.

Sugawara, Y., R. Ando, H. Kamioka, Y. Ishihara, S. A. Murshid, K. Hashimoto, N. Kataoka, K. Tsujioka, F. Kajiya, and T. Yamashiro. 2008. The alteration of a mechanical property of bone cells during the process of changing from osteoblasts to osteocytes. *Bone* 43 (1):19-24.

Suresh, S. 2007. Biomechanics and biophysics of cancer cells. *Acta Materialia* 55 (12):3989-4014.

Tavano, F., S. Bonin, G. Pinato, G. Stanta, and D. Cojoc. 2011. Custom-built optical tweezers for locally probing the viscoelastic properties of cancer cells. *International Journal of Optomechatronics* 5 (3):234-248.

Thoumine, O., P. Kocian, A. Kottelat, and J.-J. Meister. 2000. Short-term binding of fibroblasts to fibronectin: optical tweezers experiments and probabilistic analysis. *European Biophysics Journal* 29 (6):398-408.

Trappmann, B., J. E. Gautrot, J. T. Connelly, D. G. Strange, Y. Li, M. L. Oyen, M. A. C. Stuart, H. Boehm, B. Li, and V. Vogel. 2012. Extracellular-matrix tethering regulates stem-cell fate. *Nature materials* 11 (7):642-649.

Turner, C. E. 2000. Paxillin and focal adhesion signalling. *Nature cell biology* 2 (12):E231-E236.

Van Vliet, K., G. Bao, and S. Suresh. 2003. The biomechanics toolbox: experimental approaches for living cells and biomolecules. *Acta Materialia* 51 (19):5881-5905.

Vega, F. M., and A. J. Ridley. 2008. Rho GTPases in cancer cell biology. *FEBS letters* 582 (14):2093-2101.

Vera, C., R. Skelton, F. Bossens, and L. A. Sung. 2005. 3-D nanomechanics of an erythrocyte junctional complex in equibiaxial and anisotropic deformations. *Annals of biomedical engineering* 33 (10):1387-1404.

Vogel, V., and M. Sheetz. 2006. Local force and geometry sensing regulate cell functions. *Nature reviews Molecular cell biology* 7 (4):265-275.

Wang, M. D., M. J. Schnitzer, H. Yin, R. Landick, J. Gelles, and S. M. Block. 1998. Force and velocity measured for single molecules of RNA polymerase. *Science* 282 (5390):902-907.

Wang, N., J. P. Butler, and D. E. Ingber. 1993. Mechanotransduction across the cell surface and through the cytoskeleton. *Science* 260 (5111):1124-1127.

Wang, N., K. Naruse, D. Stamenović, J. J. Fredberg, S. M. Mijailovich, I. M. Tolić-Nørrelykke, T. Polte, R. Mannix, and D. E. Ingber. 2001. Mechanical behavior in living cells consistent with the tensegrity model. *Proceedings of the National Academy of Sciences* 98 (14):7765-7770.

Wang, N., and D. Stamenović. 2000. Contribution of intermediate filaments to cell stiffness, stiffening, and growth. *American Journal of Physiology-Cell Physiology* 279 (1):C188-C194.

Wang, N., I. M. Tolić-Nørrelykke, J. Chen, S. M. Mijailovich, J. P. Butler, J. J. Fredberg, and D. Stamenović. 2002. Cell prestress. I. Stiffness and prestress are closely associated in adherent contractile cells. *American Journal of Physiology-Cell Physiology* 282 (3):C606-C616.

Wen, Q., and P. A. Janmey. 2013. Effects of non-linearity on cell–ECM interactions. *Experimental cell research* 319 (16):2481-2489.

Wirtz, D., K. Konstantopoulos, and P. C. Searson. 2011. The physics of cancer: the role of physical interactions and mechanical forces in metastasis. *Nature Reviews Cancer* 11 (7):512-522.

Wojciak-Stothard, B., and A. J. Ridley. 2003. Shear stress–induced endothelial cell polarization is mediated by Rho and Rac but not Cdc42 or PI 3-kinases. *The Journal of cell biology* 161 (2):429-439.

Wolf, K., and P. Friedl. 2006. Molecular mechanisms of cancer cell invasion and plasticity. *British Journal of Dermatology* 154 (s1):11-15.

Woods, A. J., M. S. Roberts, J. Choudhary, S. T. Barry, Y. Mazaki, H. Sabe, S. J. Morley, D. R. Critchley, and J. C. Norman. 2002. Paxillin associates with poly (A)-binding protein 1 at the dense endoplasmic reticulum and the leading edge of migrating cells. *Journal of Biological Chemistry* 277 (8):6428-6437.

Yang, J., and S. Nandi. 1983. Growth of cultured cells using collagen as substrate. *Int. Rev. Cytol* 81 (249):983.

Yang, N.-S., D. Kube, C. Park, and P. Furmanski. 1981. Growth of human mammary epithelial cells on collagen gel surfaces. *Cancer research* 41 (10):4093-4100.

Yehoshua, S., R. Pollari, and J. N. Milstein. 2015. Axial optical traps: a new direction for optical tweezers. *Biophysical journal* 108 (12):2759-2766.

Yeung, T., P. C. Georges, L. A. Flanagan, B. Marg, M. Ortiz, M. Funaki, N. Zahir, W. Ming, V. Weaver, and P. A. Janmey. 2005. Effects of substrate stiffness on cell morphology, cytoskeletal structure, and adhesion. *Cell motility and the cytoskeleton* 60 (1):24-34.

Yilmaz, M., and G. Christofori. 2010. Mechanisms of motility in metastasizing cells. *Molecular Cancer Research* 8 (5):629-642.

Yim, E. K., R. M. Reano, S. W. Pang, A. F. Yee, C. S. Chen, and K. W. Leong. 2005. Nanopattern-induced changes in morphology and motility of smooth muscle cells. *Biomaterials* 26 (26):5405-5413.

Yousafzai, M. S., F. Ndoye, G. Coceano, J. Niemela, S. Bonin, G. Scoles, and D. Cojoc. 2016. Substrate-dependent cell elasticity measured by optical tweezers indentation. *Optics and Lasers in Engineering* 76:27–33.

Zhang, H., and K.-K. Liu. 2008. Optical tweezers for single cells. *Journal of The Royal Society Interface* 5 (24):671-690.